

Review

# Advances in Carbon Dot-Based Ratiometric Fluorescent Probes for Environmental Contaminant Detection: A Review

Xinxin Xing<sup>1,2,\*</sup>, Zhezhe Wang<sup>1</sup> and Yude Wang<sup>1,2,\*</sup> <sup>1</sup> School of Materials and Energy, Yunnan University, Kunming 650504, China; zzwang@mail.ynu.edu.cn<sup>2</sup> Yunnan Key Laboratory of Carbon Neutrality and Green Low-Carbon Technologies, Yunnan University, Kunming 650504, China

\* Correspondence: xxing@ynu.edu.cn (X.X.); ydwang@ynu.edu.cn (Y.W.)

**Abstract:** Detecting environmental contaminants is crucial for protecting ecosystems and human health. While traditional carbon dot (CD) fluorescent probes are versatile, they may suffer from limitations like fluctuations in signal intensity, leading to detection inaccuracies. In contrast, ratiometric fluorescent probes, designed with internal self-calibration mechanisms, offer enhanced sensitivity and reliability. This review focuses on the design and applications of ratiometric fluorescent probes based on CDs for environmental monitoring. Our discussion covers construction strategies, ratiometric fluorescence principles, and applications in detecting various environmental contaminants, including organic pollutants, heavy metal ions, and other substances. We also explore associated advantages and challenges and provide insights into potential solutions and future research directions.

**Keywords:** carbon dots; ratiometric fluorescence; environmental monitoring; contaminant detection



**Citation:** Xing, X.; Wang, Z.; Wang, Y. Advances in Carbon Dot-Based Ratiometric Fluorescent Probes for Environmental Contaminant Detection: A Review. *Micromachines* **2024**, *15*, 331. <https://doi.org/10.3390/mi15030331>

Academic Editors: Massimo Cazzanelli and Rodrigo Martinez-Duarte

Received: 15 November 2023

Revised: 22 February 2024

Accepted: 26 February 2024

Published: 28 February 2024



**Copyright:** © 2024 by the authors. Licensee MDPI, Basel, Switzerland. This article is an open access article distributed under the terms and conditions of the Creative Commons Attribution (CC BY) license (<https://creativecommons.org/licenses/by/4.0/>).

## 1. Introduction

Environmental contamination, arising from a multitude of sources such as industrial processes, urbanization, and agricultural activities, poses a significant concern for the planet's well-being [1]. This contamination includes a broad range of hazardous substances, such as organic pollutants, heavy metal ions, and biological species, each presenting unique challenges and threats to ecosystems and public health. Efforts to address environmental contamination hinge on the crucial necessity for precise and efficient detection and monitoring methods. Existing approaches, such as inductively coupled plasma mass spectrometry (ICP-MS) [2–4], atomic absorption spectrometry (AAS) [5–8], high-performance liquid chromatography (HPLC) [9–11], and surface-enhanced Raman spectroscopy (SERS) [12,13], have limitations including variable selectivity, sensitivity, and, in some cases, cumbersome analytical procedures. These conventional techniques often require complex sample preparation, time-consuming procedures, and expensive instrumentation, making them less suitable for real-time monitoring and in situ applications. The demand for more advanced and reliable techniques has never been more urgent, especially given the growing global environmental challenges. This urgency necessitates innovative solutions that can address the limitations of existing methods and provide accurate, sensitive, and practical means of environmental monitoring.

Ratiometric fluorescent probes play a crucial role in environmental monitoring, offering precise and reliable detection of various contaminants. Several ratiometric technologies are available, including Fluorescence Resonance Energy Transfer (FRET) [14], Chemiluminescence (CL) [15], Photoacoustic (PA) [16], Bioluminescence (BL) [17], and Afterglow [18], each with its own set of advantages and limitations. For example, FRET provides high sensitivity and resolution but requires matching fluorescent moieties and operates within limited distance ranges. CL, on the other hand, offers high sensitivity and rapid detection but may suffer from background signals and limited specificity. PA imaging offers deep tissue penetration and high resolution but may be hindered by slow imaging speeds and

signal attenuation. BL is advantageous for its label-free detection and suitability for in vivo imaging but faces challenges with background noise and tissue penetration depth. After-glow technology provides long-lasting signals for prolonged tracking and in vivo imaging but may lack sensitivity and resolution.

In contrast, carbon dot (CD)-based ratiometric fluorescent probes offer a promising alternative. Their dual emission peaks enable inherent self-calibration, ensuring precise and selective detection of environmental contaminants [19–24]. This property stems from the unique structural and surface characteristics of carbon dots, which facilitate efficient photon emission through mechanisms like quantum confinement and surface passivation [25]. The broad emission spectrum of CDs allows for fluorescence emission across various wavelengths, enhancing their versatility in detecting different analytes with diverse fluorescence properties [26,27]. Furthermore, CDs demonstrate remarkable fluorescence stability under diverse environmental conditions, such as exposure to light, temperature changes, and chemical environments. This stability ensures reliable and consistent fluorescence signals during environmental monitoring applications. The multiple emissive centers on the surface of CDs contribute to their unique emission peaks, providing a foundation for precise and selective detection of various contaminants [28,29]. Additionally, factors like pH [30], solvent polarity [31], and surface functionalization [32] can modulate the fluorescence intensity of CDs, further expanding their applicability in environmental sensing. CDs' dual emission peaks serve as an intrinsic self-calibration mechanism, offering precise and selective detection of various contaminants [33–43]. This unique feature positions CDs as promising candidates for advanced environmental contaminant detection, offering a solution to the limitations of traditional fluorescent probes. However, CD-based ratiometric fluorescent probes, while promising, also have limitations. These may include issues related to photobleaching, signal stability, and potential interference from background fluorescence, necessitating further investigation and optimization.

Despite numerous studies [7,44–56] and reviews [57–63] on CD-based ratiometric fluorescent probes, a comprehensive review dedicated to their role in environmental contaminant detection is notably absent. In this review, we highlight the unique potential of ratiometric fluorescent probes based on CDs for environmental monitoring. We first explore their construction strategies and the underlying principles of ratiometric fluorescence. Our discussion encompasses their diverse applications in detecting various environmental contaminants, including organic pollutants, heavy metal ions, and other contaminants. We also delve into the associated benefits and challenges, emphasizing the need for improved selectivity, sensitivity, and real-time monitoring. Additionally, we offer insights into potential solutions and future research directions, considering aspects such as probe stability and expanding analyte detection capabilities. Through this comprehensive review, we aim to contribute to the promotion of environmental safety and the advancement of sensing technology.

## 2. Construction Strategies of CDs in Detecting Environmental Contaminants

The construction of ratiometric fluorescent probes based on CDs can be categorized into various strategies, including surface modification, integration of composite materials, simple mixing strategy, and dual emission techniques. This section provides a comprehensive overview of how each strategy contributes to enhancing the performance of CDs in detecting environmental contaminants.

### 2.1. Surface Modification Strategy

Surface modification is a fundamental approach to enhance the properties of CDs to meet the specific requirements of environmental contaminant detection. By strategically altering CD surfaces, such as optimizing surface charge to enhance aqueous dispersibility or attaching specific ligands to target particular contaminants, surface modification provides a versatile means to fine-tune CDs for optimal performance. This adaptability makes surface

modification a cornerstone strategy, enabling researchers to effectively address solubility, selectivity, and stability issues.

Chemical surface modification introduces various functional groups onto CD surfaces to enhance solubility, reactivity, and specific ligand conjugation [64–73] (Figure 1a). For instance, Xu et al. [74] reported a ratiometric CD pH sensor enriched with amino groups, enabling them to specifically target lysosomes within living cells. The CDs were functionalized with abundant amino groups during their synthesis, exhibiting dual emission bands at 439 and 550 nm under single-wavelength excitation without the need for additional labeling. This sensor demonstrates robust lysosomal targeting, as evidenced by high Pearson’s colocalization coefficients (0.935 and 0.924), which indicate the degree of spatial overlap between the fluorescent signals emitted by the CDs and the lysosomal markers. Wang et al. [75] developed a novel ratiometric fluorescent probe for dipicolinic acid (DPA) point-of-care testing (POCT) by functionalizing CDs containing carboxyl and amino groups with Eu(III) ions (CDs-Eu) (Figure 1b). This approach features an exceptional detection limit of 0.8 nM.

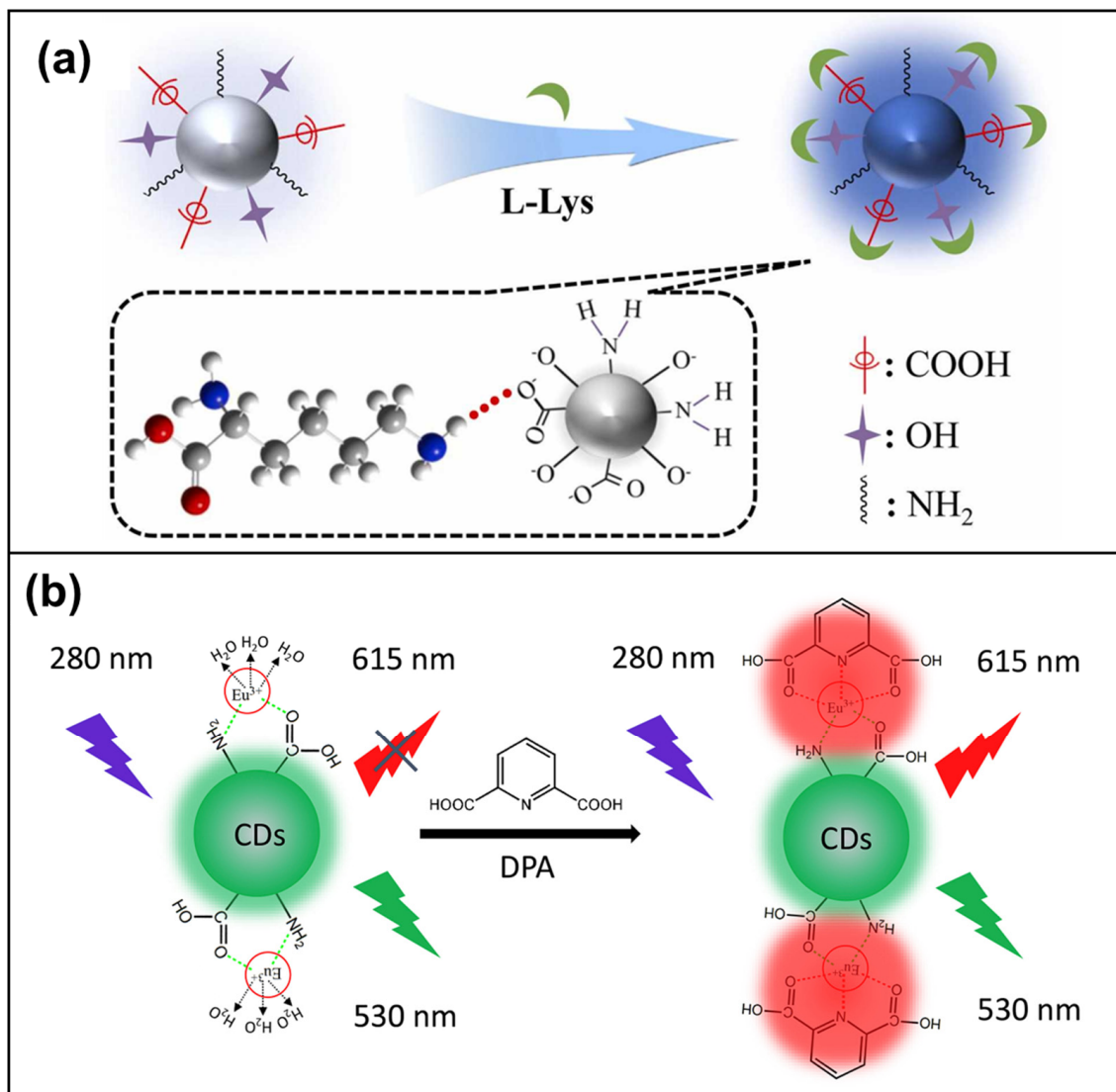


**Figure 1.** (a) Schematic of proposed route for carboxyl-, hydroxyl-, and amino groups-functionalized CDs for the detection of L-Lysine [64]; (b) schematic illustration of the carboxyl- and amino groups-functionalized CD probe for the detection of DPA [75].

Biological surface modification utilizes biomolecules like proteins, DNA, and enzymes to modify CDs, enabling the creation of highly selective probes for specific environmental pollutants or biological markers. Bu et al. [76] combined red-emitting DNA-templated copper nanoclusters (CuNCs) with blue-emitting CDs, forming a self-assembled complex known as DNA-CuNC/CDs through electrostatic forces. This complex serves as a dually emitting ratiometric probe for simultaneously detecting arginine and acetaminophen, with detection limits of 0.35  $\mu\text{M}$  and 0.26  $\mu\text{M}$ , respectively. Hu et al. [77] introduced a straightforward technique for fabricating vesicle-like CDs (VCDs) by dry heating surfactant solutions. Similar to many previously reported CDs, these VCDs display intriguing fluorescence properties. The incorporation of enzymes and gold nanoclusters (AuNCs) within the VCDs enables the development of fluorescent probes for quantifying diverse substrates, offering significant advantages in sensitivity and selectivity.

## 2.2. Composite Strategy

The composite strategy involves integrating CDs with other nanomaterials like metal nanoparticles, quantum dots, or other nanomaterials, to enhance their performance as fluorescent probes. This integration occurs through chemical bonding or interactions, resulting in a new composite material. Consequently, these composite probes display improved fluorescence characteristics, greater stability, and heightened sensitivity, making them valuable tools for environmental contaminant detection and other analytical applications.

A commonly employed strategy involves amalgamating CDs with other optical materials featuring unsaturated sites [78,79]. For instance, Zhou et al. [79] synthesized the CDs-PCN-224 (porphyrin-based metal-organic framework nanoparticles) fluorescent probe by post-synthetically modifying luminescent metal-organic frameworks and CDs. They combined the abundant groups on the surface of CDs with the unsaturated sites provided by the activated PCN-224 (Figure 2a). In this probe, the fluorescence of CDs served as a reference signal, while the fluorescence of PCN-224 acted as a highly sensitive response signal with active sites designed for detecting copper ions. The CDs-PCN probe exhibited rapid, sensitive, and selective response to copper ions, boasting an impressively low detection limit of 44 nM.

A core-shell structure is also a frequently adopted approach to protect the sensing capabilities of CDs fluorescent probes [80–85]. For example, Gong et al. [80] reported a novel and stable ratiometric fluorescent probe (B-CDs@SiO<sub>2</sub>@GSH-AuNCs/Ag<sup>+</sup>) designed for the sensitive detection of uranyl in water (Figure 2b). This probe exhibited exceptional stability, with the  $F/F_{440}$  ratio decreasing by merely 4.73% even after three months in a chloroacetic acid-sodium acetate buffer solution (pH 3.0).

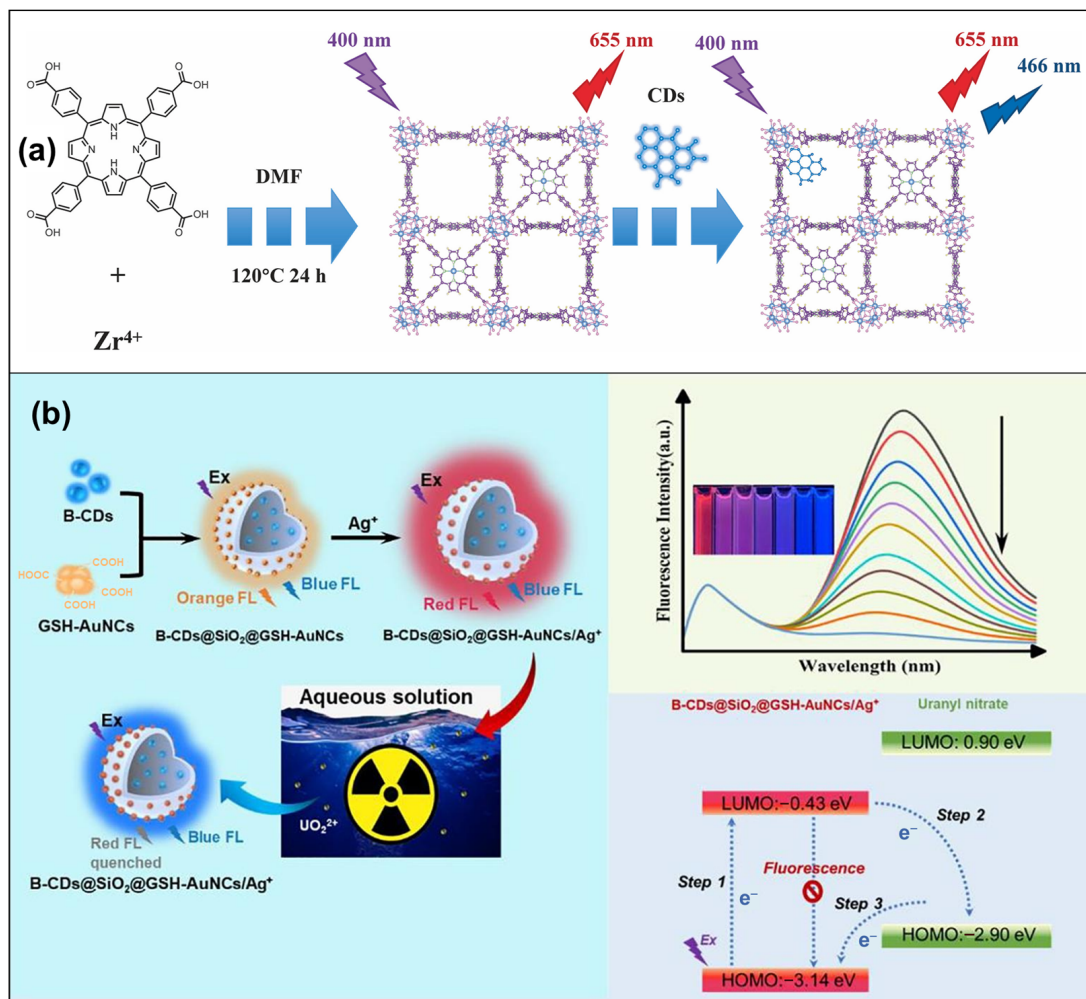


**Figure 2.** (a) Process for the solvothermal synthesis of PCN-224 and the PSM of PCN-224 with CDs [79]; (b) the preparation process of B-CDs@SiO<sub>2</sub>@GSH-AuNCs/Ag<sup>+</sup> and the schematic diagram of the detection of UO<sub>2</sub><sup>2+</sup> [80].

### 2.3. Simple Mixing Strategy

The simple mixing strategy involves the direct physical combination of CDs with other components without covalent bonding or strong interactions between them. This method offers a rapid and convenient approach to creating ratiometric fluorescent probes for environmental contaminant detection. CDs are physically mixed with other reference luminescent materials, such as polymers, nanoparticles, or other fluorophores, to establish a dual-emission system [67,86–97] (Figure 3a).

The adaptability of the simple mixing strategy facilitates the creation of ratiometric fluorescent probes tailored for various environmental contaminant detection scenarios. Through the selection of suitable companion materials and precise adjustment of mixing ratios, this method can be personalized to target specific analytes or adapt to a broad spectrum of environmental conditions. Additionally, the resulting probes can often be produced rapidly, making them attractive for applications requiring rapid response times, such as on-site monitoring and point-of-care testing. Ghasemi et al. [86] devised a ratiometric fluorescent probe composed of blue-emissive CDs (BCDs) in combination with thioglycolic acid (TGA)-capped yellow-emissive cadmium telluride (CdTe) quantum dots (YQDs). This probe demonstrates dual emissions, peaking at 443 and 560 nm, with a single excitation wavelength of 360 nm. Upon exposure to Hg(II) ions, as a representative example, the fluorescence of the YQDs undergoes selective quenching and redshift, leading to a continuous change in the probe's emission color. This transition ranges from vibrant

green to lighter shades of green, yellow-green, and yellow, eventually shifting towards warmer tones such as orange, pink, purple, weak blue, and even dark blue. The fluorescent ratiometric probe exhibits an impressively low detection limit of 4.6 nM. Qin et al. [88] developed a ratiometric fluorescence probe that combines green CDs with CdTe QDs, enabling highly selective and quantitative detection of methyl parathion (MP) (Figure 3b,c). Under alkaline conditions, MP undergoes rapid hydrolysis, yielding p-nitrophenol (p-NP). This immediate chemical transformation triggers the reinforcement of hydrogen bonds, creating an internal filter effect between the CDs and p-NP. Consequently, this interaction quenches the green fluorescence, resulting in a vivid and instant transition from green to red emission. The probe demonstrates an impressive level of sensitivity, with a detection limit as low as 8.9 nM.

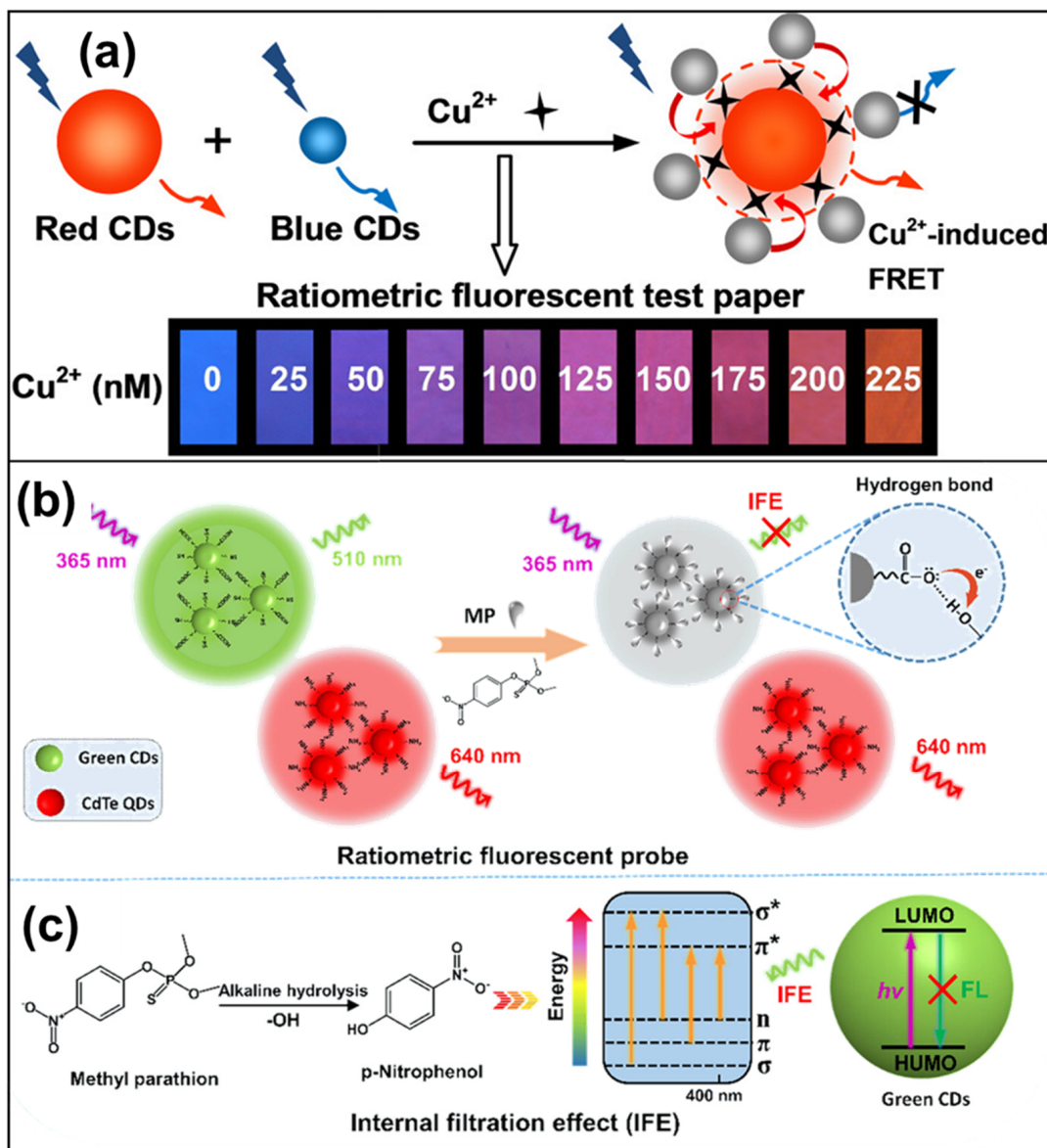


**Figure 3.** (a) Dual-colored CD ratiometric fluorescent test paper for the semiquantitative assay of Cu<sup>2+</sup> [92]; (b) integration of green CDs and CdTe quantum dots for highly selective quantitative detection of MP [88]; (c) sensing mechanism of internal filtration effect (IFE) of p-NP to green CDs (\* represents the excited state) [88].

#### 2.4. Dual Emission Strategy

The dual emission strategy is a versatile and effective approach that capitalizes on the intrinsic fluorescence properties of CDs. In this method, CDs are engineered or modified to emit light at two distinct wavelengths under the excitation of a single wavelength [64,66,67,74,98–107] (Figure 4). These dual-emitting CDs offer a built-in reference signal, enhancing the accuracy and reliability of ratiometric measurements. The concept behind dual-emitting CDs involves generating two distinct fluorescence signals within a single nanomaterial. One of these emissions typically serves as the analyte-specific response signal, while the other serves as a constant reference signal. The reference signal remains unaffected by environmental changes, making it an ideal internal standard for calibration and quality control [64,67,103–107].

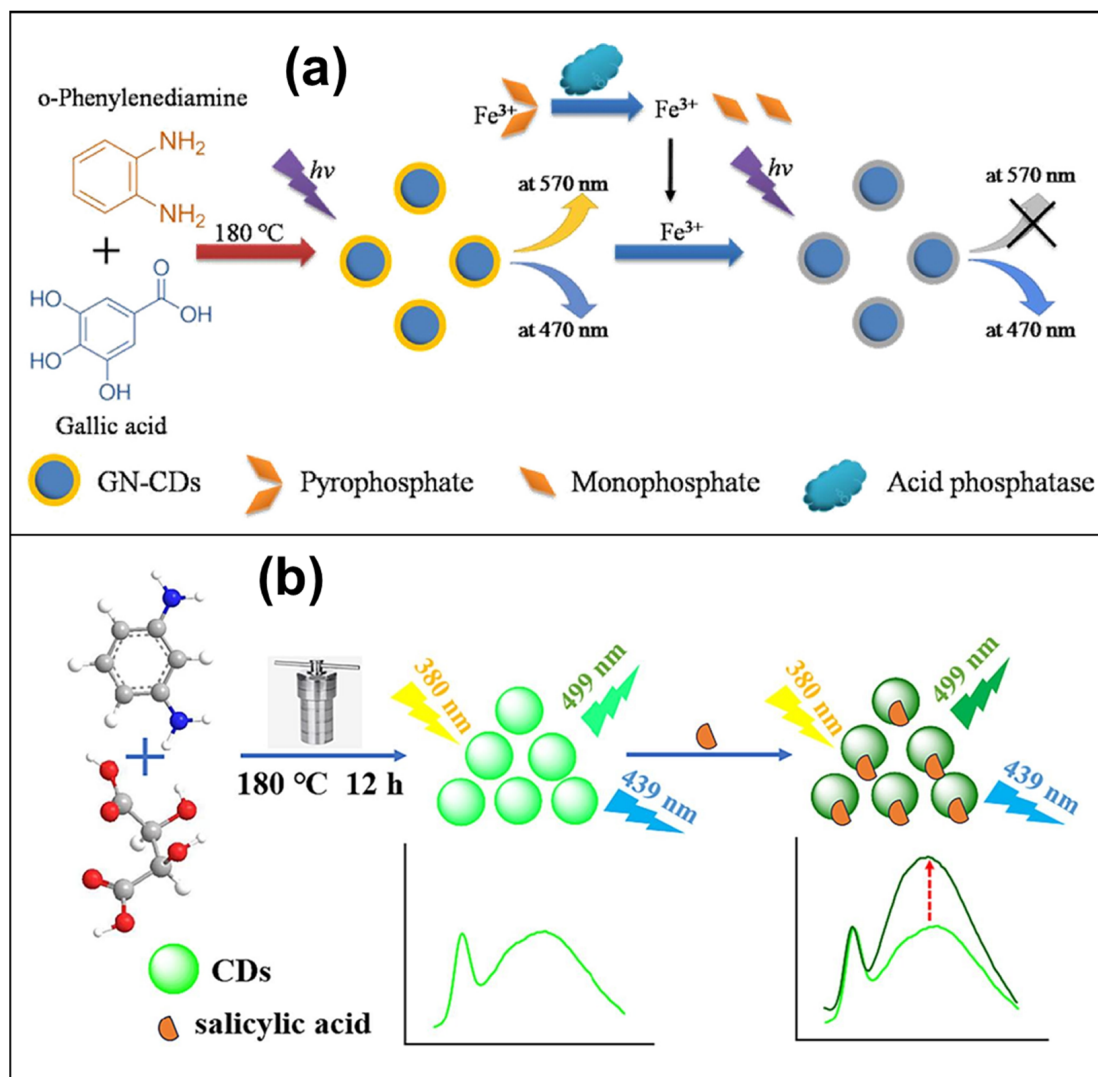


**Figure 4.** (a) Gallic acid and o-phenylenediamine were used as raw materials to prepare dual-emission CDs exhibiting two fluorescent emission peaks at 470 and 570 nm, respectively [104]; (b) the CDs, synthesized using tartaric acid (TA) and m-phenylenediamine (mPD) through a straightforward one-step hydrothermal method, display two fluorescence emission peaks at 499 nm and 439 nm when excited at 380 nm [105].

This built-in reference signal significantly enhances the accuracy and reliability of ratiometric measurements in detecting environmental contaminants. It helps alleviate potential sources of error, such as fluctuations in excitation intensity or variations in

sample matrix composition. Furthermore, the dual emission strategy allows for real-time monitoring of changes in analyte concentration or environmental conditions, making it particularly advantageous for on-site and in situ applications. Paydar et al. [98] modified CDs through a simple chemical surface modification using glutathione. The modified CDs displayed a unique spectral profile characterized by two distinctive emission peaks, separated by 170 nm, ranging from 522 to 692 nm. This probe not only enabled precise quantification of  $\text{Pb}^{2+}$  but also exhibited remarkable sensitivity, with a detection limit of  $\text{Pb}^{2+}$  as low as 2.7 nM. Chen et al. [99] introduced a near-infrared ratiometric fluorescent probe based on nitrogen and sulfur co-doped CDs (N, S-CDs). This probe was synthesized using a hydrothermal approach, employing glutathione and formamide as precursors. The N, S-CDs, due to their nitrogen and sulfur atom doping, readily form complexes with  $\text{Zn}^{2+}$ . Under excitation at 415 nm, the ratio ( $I_{650}/I_{680}$ ) of fluorescence intensity at 650 nm to 680 nm exhibited a direct correlation with the concentrations of  $\text{Zn}^{2+}$ . The probe demonstrated a remarkable detection limit of 5.0 nM for  $\text{Zn}^{2+}$ .

### 3. Application in Environmental Monitoring

Detecting environmental contaminants presents unique challenges due to the diverse nature of pollutants and their potential harm to ecosystems and human health. Traditional analytical methods often lack the sensitivity, selectivity, and real-time monitoring capabilities needed for effective environmental assessment. The application of ratiometric fluorescence principles in contaminant detection using CDs has emerged as a powerful analytical approach. CDs' ratiometric fluorescence offers a compelling solution by leveraging the inherent optical properties of CDs to address these challenges. In this approach, CDs are strategically modified or functionalized to interact specifically with target pollutants. The presence of environmental contaminants triggers changes in the CD emission properties, leading to alterations in dual-emission characteristics. These changes form the basis for ratiometric measurements, enabling the quantification of contaminant levels and differentiation of target pollutants from potential interferents. This method has practical applications in various environmental monitoring scenarios, including the detection of organic pollutants, heavy metals, and other harmful substances.

#### 3.1. Heavy Metal Ion Sensing

The detection and quantification of heavy metal ions in the environment are crucial due to their high toxicity and potential adverse effects on ecosystems and human health. Heavy metal ions, such as mercury ( $\text{Hg}^{2+}$ ) [86,101,108–115], lead ( $\text{Pb}^{2+}$ ) [67,98,106,116–119], chromium ( $\text{Cr}^{6+}$ ) [120–123], copper ( $\text{Cu}^{2+}$ ) [67,79,92,109,119,124–130], and silver ( $\text{Ag}^+$ ) [78, 117,131–133], can contaminate water, soil, and air through various industrial processes and human activities. Table 1 summarizes sensing of some heavy metal ions using CD-based ratiometric fluorescence probes. CDs have proven to be versatile tools for the sensitive and selective detection of heavy metal ions. The application of CD-based ratiometric fluorescence probes in heavy metal ion sensing relies on specific interactions between CDs and metal ions, resulting in changes in the CD emission properties.

The mechanisms underlying the detection of heavy metal ions using CD-based ratiometric fluorescence probes vary depending on the specific interactions between CDs and the metal ions. These interactions can be broadly categorized into four mechanisms: chelation, surface modification, quenching, and aggregation-induced changes.

Functionalized CDs with specific ligands or receptors have the unique ability to form stable complexes with heavy metal ions through chelation. This involves binding metal ions to functional groups on the CD surface, creating enduring chemical bonds (Figure 5a). As a result, this chelation process induces significant alterations in the CDs' emission properties, allowing for precise detection of metal ions such as  $\text{Hg}^{2+}$  [112],  $\text{Pb}^{2+}$  [106], and  $\text{Cu}^{2+}$  [124]. This mechanism is widely used in environmental monitoring, especially in assessing water and soil quality due to its high sensitivity and selectivity.



**Table 1.** A summary of CD-based ratiometric fluorescence probes for the detection of heavy metal ions.

| Ratiometric FL Probes       | Construction Strategy          | Analyte          | LOD                       | Ref.  |
|-----------------------------|--------------------------------|------------------|---------------------------|-------|
| ZIF-8@g-CNQD/CdTe           | Quench of CdTe                 | Hg <sup>2+</sup> | ~46 nM                    | [111] |
| Ag/Au@CDs nanohybrids       | Ligand effect                  | Hg <sup>2+</sup> | 7 nM                      | [109] |
| YQDs + BCDs                 | Quench of CdTe                 | Hg <sup>2+</sup> | 4.6 nM                    | [86]  |
| Dual-emissive CDs           | Ligand effect                  | Hg <sup>2+</sup> | 0.27 μM                   | [101] |
| (NCDs-RhB@COF               | Ligand effect                  | Hg <sup>2+</sup> | 15.9 nM                   | [108] |
| CDs and CdSe@ZnS QDs        | Quench of CdSe@ZnS QDs         | Hg <sup>2+</sup> | 0.1 μM                    | [112] |
| CDs and Si NCs              | Quench of Si NCs               | Hg <sup>2+</sup> | 7.63 nM                   | [110] |
| CuNCs-CNQDs                 | Aggregation of CuNCs           | Pb <sup>2+</sup> | 0.0031 mg L <sup>-1</sup> | [116] |
| N-CDs/AuNCs                 | Aggregation of AuNCs           | Pb <sup>2+</sup> | 0.5 μM                    | [67]  |
| GSH-modified CDs            | Aggregation of CDs             | Pb <sup>2+</sup> | 2.7 nM                    | [98]  |
| Label-free CDs              | Ligand effect                  | Pb <sup>2+</sup> | 0.055 μM                  | [106] |
| Y-CDs                       | IFE                            | Cr <sup>6+</sup> | 2.3 nM                    | [121] |
| Dual-emissive CDs           | IFE                            | Cr <sup>6+</sup> | 0.4 μM                    | [120] |
| N-doped Dual-emissive CDs   | IFE                            | Cr <sup>6+</sup> | 3.2 μM                    | [122] |
| Ag/Au@CDs nanohybrids       | Aggregation of CDs             | Cu <sup>2+</sup> | 5 nM                      | [109] |
| N-CDs/AuNCs                 | Quench of AuNCs                | Cu <sup>2+</sup> | 0.15 μM                   | [67]  |
| N-CDs/AgNCs                 | Aggregation of N-CDs/AgNCs     | Cu <sup>2+</sup> | 0.13 μM                   | [124] |
| r-CDs and b-CDs (1:7)       | Quench of b-CDs                | Cu <sup>2+</sup> | 8.82 nM                   | [92]  |
| Dual-emissive CQDs          | Ligand effect                  | Cu <sup>2+</sup> | -                         | [130] |
| Dual-emissive N-CDs         | Ligand effect                  | Cu <sup>2+</sup> | 17.7 nM                   | [126] |
| GCDs@RSPN                   | Quench of GCDs                 | Cu <sup>2+</sup> | 0.58 μM                   | [127] |
| Dual-mode SQD-CQD probe     | IFE                            | Cu <sup>2+</sup> | 31 nM and 47 nM           | [128] |
| MPA-CdTe and CDs            | Quench of MPA-CdTe             | Cu <sup>2+</sup> | 0.36 nM                   | [125] |
| CDs-PCN                     | Ligand effect                  | Cu <sup>2+</sup> | 44 nM                     | [79]  |
| NCCOF <sub>TAPT-TT</sub>    | Photoinduced electron transfer | Cu <sup>2+</sup> | 17.3 nM                   | [129] |
| P-CDs/R-CDs                 | Quench of P-CDs                | Ag <sup>+</sup>  | 32 nM                     | [132] |
| NALC-CdTe QDs and N,Si-CQDs | Quench of NALC-CdTe QDs        | Ag <sup>+</sup>  | 1.7 nM                    | [131] |
| CSs-AuNCs                   | Increased FL of AuNCs          | Ag <sup>+</sup>  | 1.6 nM                    | [78]  |

Surface modification techniques serve as a versatile approach to engineer CDs for the selective adsorption of heavy metal ions. By leveraging various methods, including electrostatic interactions, ion exchange, or chemical binding, CDs can be tailored to adsorb specific metal ions (Figure 5b). This surface modification technique results in the adsorption of metal ions onto the CD surface, thereby altering the CD's photophysical properties. These changes enable ratiometric measurements for the detection of metal ions such as Pb<sup>2+</sup> [98] and Cu<sup>2+</sup> [109,127], which are frequently detected using this mechanism.

In certain situations, heavy metal ions directly quench the fluorescence of CDs. This quenching phenomenon arises from the binding of metal ions to CDs, causing a non-radiative energy transfer that reduces the fluorescence intensity of the CDs (Figure 5c). As a result, this quenching mechanism is employed for the detection of a wide range of metal ions, including Hg<sup>2+</sup> [86,101,108,109,112], Ag<sup>+</sup> [131,132], Cr<sup>6+</sup> [120–122], and Cu<sup>2+</sup> [67,92,126]. Its applicability extends to various fields, including clinical diagnostics and environmental monitoring, due to its simplicity and ability to yield real-time results.

The presence of heavy metal ions can induce the aggregation of CDs through interactions with the metal ions, a phenomenon often described as aggregation-induced changes. This process leads to noticeable alterations in the photophysical properties of CDs (Figure 5d). Specifically, it results in changes in the dual-emission characteristics that are used for ratiometric measurements. As such, this mechanism has found significant application in the detection of metal ions such as Cu<sup>2+</sup> [67,109,124,129] and Pb<sup>2+</sup> [67,98,116]. Its unique sensitivity to changes in the aggregation state of CDs has made it a valuable tool in the study of complex environmental samples and biological systems.

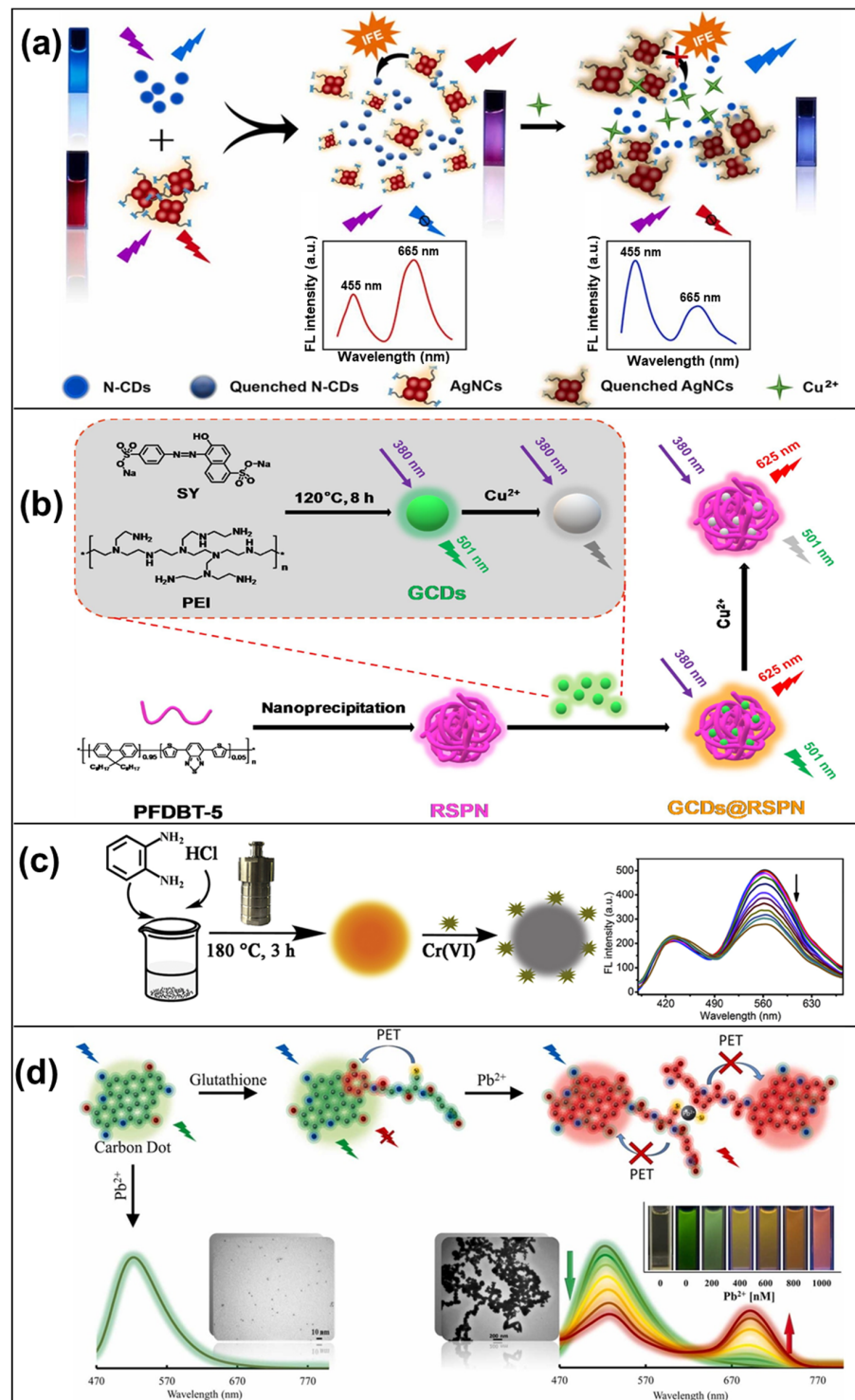


**Figure 5.** (a) Upon the introduction of  $\text{Cu}^{2+}$ , the red fluorescence of AgNCs diminishes due to the robust chelating interaction between L-glutathione and  $\text{Cu}^{2+}$ , while the blue fluorescence undergoes a resurgence, leading to a notable shift in fluorescence color from pink to blue under UV light [124]; (b) a dual-emissive fluorescent ratiometric probe for  $\text{Cu}^{2+}$  was developed by loading amine-coated CDs onto red emission semiconducting polymer nanoparticles (RSPN) through electrostatic adsorption [127]; (c) schematic illustration of Y-CDs preparation and the quenching process upon the addition of  $\text{Cr(VI)}$  to the system [121]; (d) the average dynamic size of m-AP-GSH CDs transformed from 1.67 nm without  $\text{Pb}^{2+}$  to 289.3 nm after  $\text{Pb}^{2+}$  addition, indicating significant aggregation of the CDs with  $\text{Pb}^{2+}$  [98].

### 3.2. Detection of Organic Pollutants

Detecting organic pollutants accurately and precisely is crucial for environmental monitoring because these contaminants consist of various compounds, each with distinct chemical properties and potential environmental and health impacts. Organic pollutants encompass polycyclic aromatic hydrocarbons (PAHs), pesticides, herbicides, pharmaceutical residues, industrial chemicals, and other recalcitrant organic compounds. Assessing environmental quality and ensuring public safety heavily relies on the detection and quantification of these substances.

Pesticides and herbicides pose significant challenges in environmental monitoring, and CDs offer a promising solution for their detection and sensing [134–136] (Figure 6a). Shokri et al. [134] developed a novel method to detect triticonazole using a dual-emission ratiometric fluorescence sensor. This sensor involved encapsulating boron-doped CDs (B-CDs) with blue fluorescence and phosphorus-doped green-emitting CDs (P-CDs) into a zeolitic imidazolate framework-8 (ZIF-8). The B-CDs/P-CDs@ZIF-8 composite displayed two distinct emission peaks at 440 nm and 510 nm when excited at a single wavelength of 385 nm, corresponding to B-CDs and P-CDs, respectively. In the presence of triticonazole, the fluorescence intensity of B-CDs decreased significantly, while that of P-CDs remained constant. As the concentration of triticonazole increased, the color of the ratiometric probe shifted gradually from blue to green. Under optimized conditions, the B-CDs/P-CDs@ZIF-8 probe exhibited a low detection limit of 4.0 nM for triticonazole.

Pharmaceutical residues can disrupt ecosystems, contribute to antibiotic resistance, and lead to various health issues, including allergies and poisoning. Monitoring and controlling pharmaceutical residues are crucial to mitigate these risks [65,69,81,88,105,137–150] (Figure 6b). One fundamental mechanism in detecting pharmaceutical residues is related to electron transfer processes. Adsorption of pharmaceutical residues onto the surfaces of CDs can trigger electron transfer processes, resulting in alterations in the CDs' emission properties. Jalili et al. [141] introduced a rapid-response ratiometric probe for the sensitive visual detection of the banned veterinary antibiotic chloramphenicol (CLP), which is still illicitly used in animal husbandry. They utilized two kinds of CDs, one with yellow emission (Y/CDs, 560 nm) as the target-sensitive component and the other with blue emission (B/CDs, 440 nm) as reference dyes to create the ratiometric fluorescence probe (mMIP@YBCDs). In the presence of CLP, interactions between amino groups ( $-NH_2$ ) in the APTES molecule, located within the binding sites of mMIP@YBCDs, and functional groups in CLP, such as the carbonyl and nitro groups, lead to the formation of a Meisenheimer complex through hydrogen bonding. This interaction results in electron transfer between Y/CDs and CLP, significantly inhibiting radiative recombination of the electron–hole pair. Consequently, the majority of excited electrons return to the ground state via nonradiative decay instead of radiative decay, causing a reduction in fluorescence intensity.

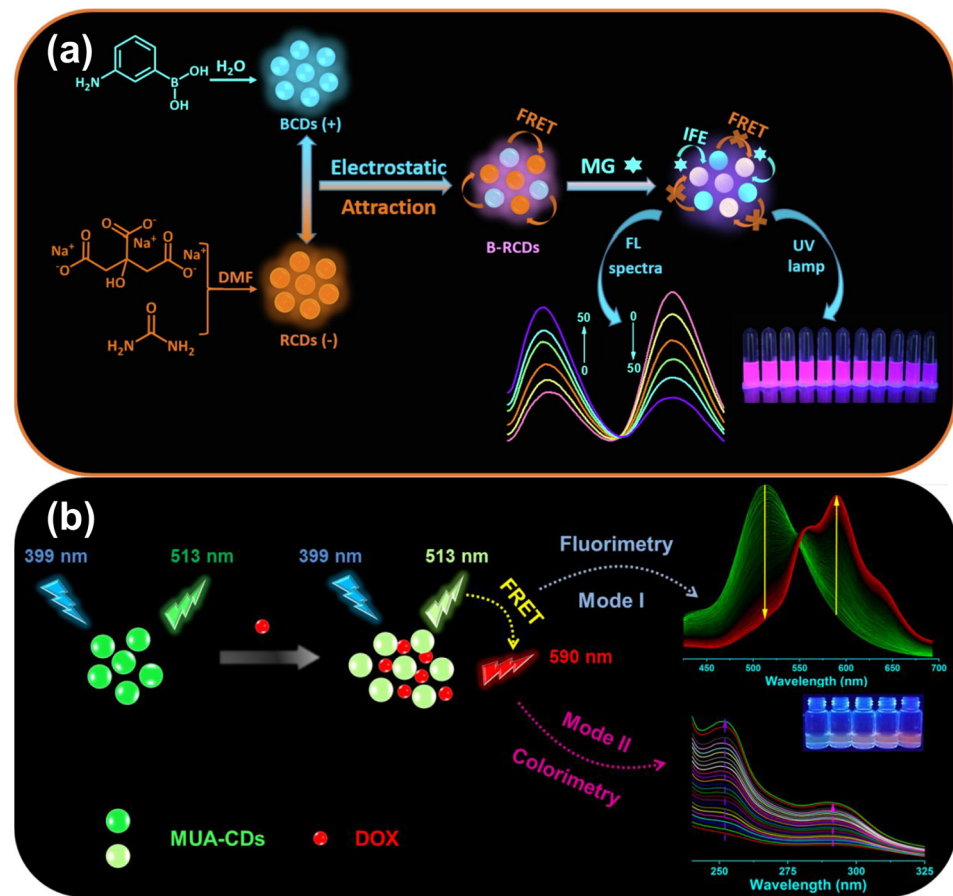


**Figure 6.** (a) Schematic diagram of construction method for blue/red-emission CDs probe and ratiometric response to malachite green [135]. (b) Illustration of 11-mercaptoundecanoic acid-functionalized CDs as a ratiometric fluorescence probe for selective doxorubicin (DOX) detection. Mode I displays the fluorescence spectra of mercaptoundecanoic-CDs (MUA-CDs) (0.2 mg/mL) under excitation at 399 nm, responding to varying DOX concentrations (0.25–97.07  $\mu\text{M}$ ). Mode II exhibits the UV-vis absorption spectra of MUA-CDs under different DOX concentrations (0–63.20  $\mu\text{M}$ ) [148].

### 3.3. Other Contaminants

In addition to organic pollutants and heavy metal ions, CD-based ratiometric fluorescence probes have been utilized in detecting various other environmental contaminants. These contaminants consist of a diverse range of substances, each presenting unique challenges for detection and quantification. The versatility and adaptability of CD-based probes make them well-suited for addressing these challenges.

**Anions:** CD-based probes have been employed for detecting various anions, including phosphate (Pi) [87,103,151], nitrite ( $\text{NO}_2^-$ ) [68,152], hypochlorite ( $\text{ClO}^-$ ) [153,154], bisulfite [155], and sulfide ( $\text{S}^{2-}$ ) [156] in water sources, facilitating the assessment of water quality.

**Gases and Vapors:** CD-based sensors have been developed for detecting gases such as oxygen ( $\text{O}_2$ ) [157], hydrogen sulfide ( $\text{H}_2\text{S}$ ) [66,158], volatile organic compounds (VOCs) [122,159–161] (Figure 7a,b), and nitrogen dioxide ( $\text{NO}_2$ ) [162] (Figure 7c) in liquid or air quality monitoring scenarios.

**Biological and Biomolecular Targets:** CD-based ratiometric fluorescence probes have been adapted for detecting specific biological and biomolecular targets, such as bacteria [82,163,164], biomarkers [75,165], cholesterol [77], amino acids [64], guanine [166,167], DNA [168] (Figure 7d,e), and proteins [1,91,107,169,170]. These probes find applications in genomics, molecular diagnostics, and bioanalytical assays.

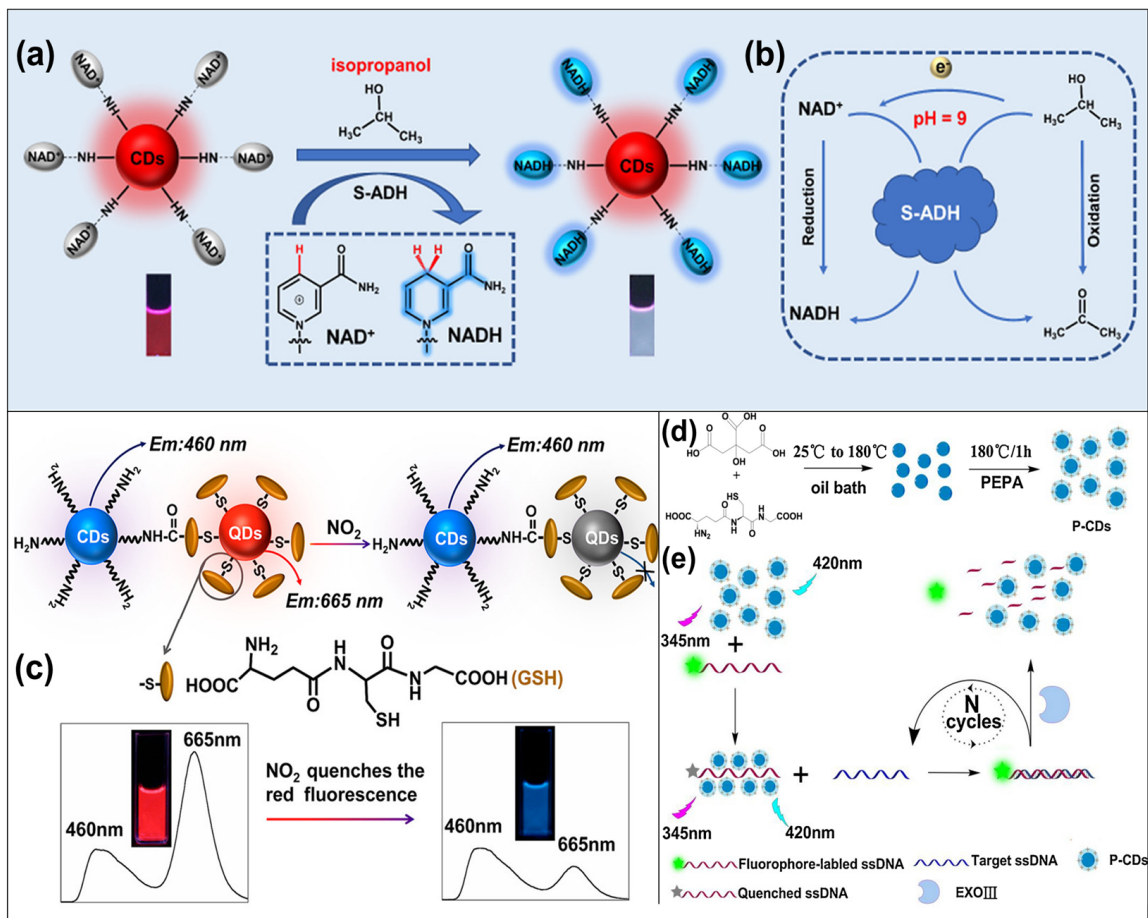


**Figure 7.** (a) Schematic diagram of the ratiometric fluorescence sensing system for isopropanol detection and (b) reaction mechanism of the probe sensing part nicotinamide adenine dinucleotide (NAD<sup>+</sup>) for isopropanol [161]; (c) schematic illustration of blue-emission CDs and red-emission CdTe QDs hybrid probe structure and the visual detection principle for NO<sub>2</sub> [162]; (d) synthesis of positive-charged CDs (P-CDs) in a two-step procedure; (e) the quenching of fluorophore-labelled ssDNA by P-CDs, while retaining the stable fluorescence intensity of P-CDs, enabling a ratiometric analytical method for *Gardnerella vaginalis* DNA with the target sequence circulating under the assistance of exonuclease III (Exo III) [168].

#### 4. Conclusions and Outlook

Detecting environmental contaminants is crucial for safeguarding ecosystems and public health. While traditional CD fluorescent probes have shown versatility in environmental monitoring, they are not without limitations, particularly in terms of the accuracy and reliability of detection results due to fluctuations in absolute signal intensity. Ratiometric fluorescent probes, engineered with internal self-calibration mechanisms, offer significant advantages, including enhanced sensitivity and reliability. In this review, we have explored the design and applications of ratiometric fluorescent probes based on CDs for environmental monitoring. Our discussion has covered construction strategies, ratiometric fluorescence principles, and applications in detecting various environmental contaminants, including organic pollutants, heavy metal ions, and other environmental threats. Additionally, we have outlined future directions as follows:

- I. Sustainable synthesis of biocompatible CDs for eco-friendly sensing: Most CDs are made using non-renewable materials and energy-intensive methods, which harm the environment. Additionally, biocompatible CDs are a new area with limited practical uses. Creating biocompatible CDs supports the global shift towards green chemistry and sustainability. These CDs can reduce environmental risks, making sensing appli-

cations safer. Their use also cuts down on hazardous waste and promotes renewable resources.

- II. Multiplexed sensing for comprehensive environmental analysis: Currently, many CD-based ratiometric probes are designed for single analytes, which makes combining multiple sensing capabilities into one probe challenging due to possible cross-reactivity. Since the environment usually has a mix of contaminants, creating multiplexed ratiometric probes is crucial. These probes can detect various contaminants simultaneously, reducing the need for many sensors. This approach provides a more accurate assessment of environmental conditions by handling the complex nature of contaminants.
- III. Portable field sensors for real-time monitoring: While CD-based ratiometric sensors are mainly used in labs, their usefulness in field applications is limited. Even portable sensors may lack durability and quick detection capabilities. Portable sensors are important for real-time monitoring in tough environmental conditions, enabling rapid responses to emergencies. Field monitoring ensures timely environmental assessments and responses, especially in remote or disaster-prone areas. Developing portable, strong sensors is vital for improving data collection.
- IV. Microscale environmental mapping for detailed insight: Microscale environmental mapping using CD-based ratiometric fluorescence has limitations in spatial precision and integrating diverse sensing technologies. Many environmental issues require a microscale perspective for deep understanding. Integrated spatial data improve decision-making. Enhanced spatial precision offers detailed insight into contamination patterns. Collaboration across disciplines helps interpret data effectively and derive actionable insights.

**Author Contributions:** Writing—review and editing, X.X.; investigation, Z.W.; writing—original draft preparation, Y.W. All authors have read and agreed to the published version of the manuscript.

**Funding:** This work was funded by the fellowship of China Postdoctoral Science Foundation (2021M690555). This work was also supported by the National Natural Science Foundation of China (No. 41876055 and 61761047), the Yunnan Provincial Department of Science and Technology through the Key Project for Science and Technology (Grant No. 2017FA025), the Program for Innovative Research Team (in Science and Technology) in University of Yunnan Province, and the Project of the Department of Education of Yunnan Province (2022Y003).

**Data Availability Statement:** No applicable.

**Acknowledgments:** We gratefully acknowledge the support from the School of Materials and Energy, Yunnan University.

**Conflicts of Interest:** The authors declare no conflicts of interest.

## References

1. Li, S.; Song, X.; Wang, Y.; Hu, Z.; Yan, F.; Feng, G. Developed a ratiometric fluorescence pH nanosensor based on label-free carbon dots for intracellular lysosome imaging and water pH monitoring with a smartphone. *Dye. Pigment.* **2021**, *193*, 109490. [[CrossRef](#)]
2. Hsu, W.H.; Jiang, S.J.; Sahayam, A.C. Determination of Cu, As, Hg and Pb in vegetable oils by electrothermal vaporization inductively coupled plasma mass spectrometry with palladium nanoparticles as modifier. *Talanta* **2013**, *117*, 268–272. [[CrossRef](#)]
3. Liu, M.; Hashi, Y.; Pan, F.; Yao, J.; Song, G.; Lin, J. Automated on-line liquid chromatography-photodiode array-mass spectrometry method with dilution line for the determination of bisphenol A and 4-octylphenol in serum. *J. Chromatogr. A* **2006**, *1133*, 142–148. [[CrossRef](#)]
4. Zhou, J.; Tian, Y.; Wu, X.; Hou, X. Visible light photochemical vapor generation using metal-free g-C<sub>3</sub>N<sub>4</sub>/CQDs composites as catalyst: Selective and ultrasensitive detection of mercury by ICP-MS. *Microchem. J.* **2017**, *132*, 319–326. [[CrossRef](#)]
5. Huang, Y.; Peng, J.; Huang, X. Allylthiourea functionalized magnetic adsorbent for the extraction of cadmium, copper and lead ions prior to their determination by atomic absorption spectrometry. *Microchim. Acta* **2019**, *186*, 51. [[CrossRef](#)] [[PubMed](#)]
6. Saber Tehrani, M.; Rastegar, F.; Parchehbaf, A.; Rezvani, Z. Determination of copper by flame atomic absorption spectrometry after preconcentration with activated carbon impregnated with a new Schiff base. *Chin. J. Chem.* **2005**, *23*, 1437–1442. [[CrossRef](#)]
7. Li, Y.K.; Yang, T.; Chen, M.L.; Wang, J.H. Supported carbon dots serve as high-performance adsorbent for the retention of trace cadmium. *Talanta* **2018**, *180*, 18–24. [[CrossRef](#)]

8. Mashkani, M.; Mehdinia, A.; Jabbari, A.; Bide, Y.; Nabid, M.R. Preconcentration and extraction of lead ions in vegetable and water samples by N-doped carbon quantum dot conjugated with Fe<sub>3</sub>O<sub>4</sub> as a green and facial adsorbent. *Food Chem.* **2018**, *239*, 1019–1026. [[CrossRef](#)]
9. Wu, Q.; Li, Y.; Wang, C.; Liu, Z.; Zang, X.; Zhou, X.; Wang, Z. Dispersive liquid-liquid microextraction combined with high performance liquid chromatography-fluorescence detection for the determination of carbendazim and thiabendazole in environmental samples. *Anal. Chim. Acta* **2009**, *638*, 139–145. [[CrossRef](#)]
10. Zhuang, Y.; Zhou, M.; Gu, J.; Li, X. Spectrophotometric and high performance liquid chromatographic methods for sensitive determination of bisphenol A. *Spectrochim. Acta Part A* **2014**, *122*, 153–157. [[CrossRef](#)] [[PubMed](#)]
11. Tan, X.; Song, Y.; Wei, R.; Yi, G. Determination of trace bisphenol A in water using three-phase hollow fiber liquid-phase microextraction coupled with high performance liquid chromatography. *Chin. J. Anal. Chem.* **2012**, *40*, 1409–1414. [[CrossRef](#)]
12. Hua, M.Z.; Feng, S.; Wang, S.; Lu, X. Rapid detection and quantification of 2,4-dichlorophenoxyacetic acid in milk using molecularly imprinted polymers-surface-enhanced Raman spectroscopy. *Food Chem.* **2018**, *258*, 254–259. [[CrossRef](#)] [[PubMed](#)]
13. Chen, M.; Du, B.; Wang, Q.; Zhang, J.; Zhu, X.; Lin, Z.; Dong, Y.; Fu, F.; Yu, T. Tuning the aggregation of silver nanoparticles with carbon dots for the surface-enhanced Raman scattering application. *Carbon* **2021**, *185*, 442–448. [[CrossRef](#)]
14. Ge, Y.Q.; Liu, A.K.; Ji, R.X.; Shen, S.L.; Cao, X.Q. Detection of Hg<sup>2+</sup> by a FRET ratiometric fluorescent probe based on a novel pyrido[1,2-a]benzimidazole-rhodamine system. *Sens. Actuators B Chem.* **2017**, *251*, 410–415. [[CrossRef](#)]
15. An, W.W.; Mason, R.P.; Lippert, A.R. Energy transfer chemiluminescence for ratiometric pH imaging. *Org. Biomol. Chem.* **2018**, *16*, 4176–4182. [[CrossRef](#)]
16. Fan, X.P.; Wang, H.Z.; Yang, W.; Ren, T.B.; Yuan, L. Ratiometric photoacoustic imaging of endogenous HNO in vivo for assessing prodrug release and liver injury. *Chem. Commun.* **2023**, *59*, 8969–8972. [[CrossRef](#)]
17. Van de Bittner, G.C.; Bertozzi, C.R.; Chang, C.J. Strategy for dual-analyte luciferin imaging: In vivo bioluminescence detection of hydrogen peroxide and caspase activity in a murine model of acute inflammation. *J. Am. Chem. Soc.* **2013**, *135*, 1783–1795. [[CrossRef](#)]
18. Chen, W.; Zhang, Y.; Li, Q.; Jiang, Y.; Zhou, H.; Liu, Y.H.; Miao, Q.Q.; Gao, M.Y. Near-Infrared afterglow luminescence of chlorin nanoparticles for ultrasensitive in vivo imaging. *J. Am. Chem. Soc.* **2022**, *144*, 6719–6726. [[CrossRef](#)] [[PubMed](#)]
19. Wang, Y.; Mao, L.; Liu, W.; Ding, F.; Zou, P.; Wang, X.; Zhao, Q.; Rao, H. A ratiometric fluorometric and colorimetric probe for the β-thalassemia drug deferiprone based on the use of gold nanoclusters and carbon dots. *Microchim. Acta* **2018**, *185*, 442. [[CrossRef](#)] [[PubMed](#)]
20. Farahmand Nejad, M.A.; Hormozi-Nezhad, M.R. Design of a ratiometric fluorescent probe for naked eye detection of dopamine. *Anal. Methods* **2017**, *9*, 3505–3512. [[CrossRef](#)]
21. Ma, Y.; Wang, Y.; Liu, Y.; Shi, L.; Yang, D. A cascade-triggered ratiometric fluorescent sensor based on nanocomposite for lactate determination. *Sens. Actuators B Chem.* **2022**, *355*, 131295. [[CrossRef](#)]
22. Macairan, J.R.; Jaunky, D.B.; Piekny, A.; Naccache, R. Intracellular ratiometric temperature sensing using fluorescent carbon dots. *Nanoscale Adv.* **2019**, *1*, 105–113. [[CrossRef](#)]
23. Wang, Y.; Liu, H.; Song, H.; Yu, M.; Wei, L.; Li, Z. Synthesis of dual-emission fluorescent carbon quantum dots and their ratiometric fluorescence detection for arginine in 100% water solution. *New J. Chem.* **2019**, *43*, 13234–13239. [[CrossRef](#)]
24. Xu, X.; Ren, D.; Chai, Y.; Cheng, X.; Mei, J.; Bao, J.; Wei, F.; Xu, G.; Hu, Q.; Cen, Y. Dual-emission carbon dots-based fluorescent probe for ratiometric sensing of Fe(III) and pyrophosphate in biological samples. *Sens. Actuators B Chem.* **2019**, *298*, 126829. [[CrossRef](#)]
25. Dimos, K. Carbon quantum dots: Surface passivation and functionalization. *Curr. Org. Chem.* **2016**, *20*, 682–695. [[CrossRef](#)]
26. Ostertag, B.J.; Cryan, M.T.; Serrano, J.M.; Liu, G.; Ross, A.E. Porous carbon nanofiber-modified carbon fiber microelectrodes for dopamine detection. *ACS Appl. Nano Mater.* **2022**, *5*, 2241–2249. [[CrossRef](#)]
27. Sharma, V.; Tiwari, P.; Mobin, S.M. Sustainable carbon-dots: Recent advances in green carbon dots for sensing and bioimaging. *J. Mater. Chem. B* **2017**, *5*, 8904–8924. [[CrossRef](#)] [[PubMed](#)]
28. Khan, W.U.; Zhou, P.; Qin, L.Y.; Alam, A.; Ge, Z.J.; Wang, Y.H. Solvent-free synthesis of nitrogen doped carbon dots with dual emission and their biological and sensing applications. *Mater. Today Nano* **2022**, *18*, 100205. [[CrossRef](#)]
29. Hu, Y.; Yang, Z.B.; Lu, X.; Guo, J.Z.; Cheng, R.; Zhu, L.L.; Wang, C.F.; Chen, S. Facile synthesis of red dual-emissive carbon dots for ratiometric fluorescence sensing and cellular imaging. *Nanoscale* **2020**, *12*, 5494–5500. [[CrossRef](#)] [[PubMed](#)]
30. Huang, M.J.; Liang, X.Y.; Zhang, Z.X.; Wang, J.; Fei, Y.Y.; Ma, J.; Qu, S.N.; Mi, L. Carbon dots for intracellular pH sensing with fluorescence lifetime imaging microscopy. *Nanomaterials* **2020**, *10*, 604. [[CrossRef](#)]
31. Meng, Y.; Cui, S.; Lei, P.; Guo, J.; Wang, Q.; Shuang, S.; Dong, C. Design of polarity-dependence orange emission multifunctional carbon dots for water detection and anti-counterfeiting. *Mater. Today Chem.* **2023**, *33*, 101669. [[CrossRef](#)]
32. Zhao, Q.L.; Wang, X.T.; Song, Q.H.; Zang, Z.H.; Fan, C.Y.; Li, L.L.; Yu, X.F.; Lu, Z.M.; Zhang, X.H. Electrochemical synthesis of fluorescence-enhanced carbon dots with multicolor emission via surface nitrogen and sulfur modulation for information encryption applications. *J. Mater. Chem. C* **2023**, *11*, 14439–14447. [[CrossRef](#)]
33. Bu, D.; Song, H.; Li, Z.; Wei, L.; Zhang, H.; Yu, M. Carbon-dot-based ratiometric fluorescent probe of intracellular zinc ion and persulfate ion with low dark toxicity. *Luminescence* **2020**, *35*, 1319–1327. [[CrossRef](#)] [[PubMed](#)]
34. Zhu, J.; Chu, H.; Shen, J.; Wang, C.; Wei, Y. Green preparation of carbon dots from plum as a ratiometric fluorescent probe for detection of doxorubicin. *Opt. Mater.* **2021**, *114*, 110941. [[CrossRef](#)]

35. Zhang, D.; Jia, D.; Fang, Z.; Min, H.; Xu, X.; Li, Y. The detection of anthrax biomarker DPA by ratiometric fluorescence probe of carbon quantum dots and europium hybrid material based on poly(ionic)-liquid. *Molecules* **2023**, *28*, 6557. [[CrossRef](#)] [[PubMed](#)]
36. Shi, Y.; Lin, L.; Wei, Y.; Li, W.; Nie, P.; He, Y.; Feng, X. Gold nanoparticles-mediated ratiometric fluorescence aptasensor for ultra-sensitive detection of Abscisic Acid. *Biosens. Bioelectron.* **2021**, *190*, 113311. [[CrossRef](#)] [[PubMed](#)]
37. Ma, Y.; Cen, Y.; Sohail, M.; Xu, G.; Wei, F.; Shi, M.; Xu, X.; Song, Y.; Ma, Y.; Hu, Q. A ratiometric fluorescence universal platform based on N, Cu codoped carbon dots to detect metabolites participating in H<sub>2</sub>O<sub>2</sub>-generation reactions. *ACS Appl. Mater. Interfaces* **2017**, *9*, 33011–33019. [[CrossRef](#)]
38. Shao, K.; Yang, Y.; Ye, S.; Gu, D.; Wang, T.; Teng, Y.; Shen, Z.; Pan, Z. Dual-colored carbon dots-based ratiometric fluorescent sensor for high-precision detection of alkaline phosphatase activity. *Talanta* **2020**, *208*, 120460. [[CrossRef](#)]
39. Zhang, Y.; Xu, H.; Yang, Y.; Zhu, F.; Pu, Y.; You, X.; Liao, X. Efficient fluorescence resonance energy transfer-based ratiometric fluorescent probe for detection of dopamine using a dual-emission carbon dot-gold nanocluster nanohybrid. *J. Photochem. Photobiol. A* **2021**, *411*, 113195. [[CrossRef](#)]
40. Liang, S.; Deng, X.; Fan, Y.; Li, J.; Wang, M.; Zhang, Z. A ratiometric fluorometric heparin assay based on the use of CdTe and polyethyleneimine-coated carbon quantum dots. *Microchim. Acta* **2018**, *185*, 519. [[CrossRef](#)]
41. Bao, J.; Mei, J.; Cheng, X.; Ren, D.; Xu, G.; Wei, F.; Sun, Y.; Hu, Q.; Cen, Y. A ratiometric lanthanide-free fluorescent probe based on two-dimensional metal-organic frameworks and carbon dots for the determination of anthrax biomarker. *Microchim. Acta* **2021**, *188*, 84. [[CrossRef](#)]
42. Nemati, F.; Zare-Dorabei, R. A ratiometric probe based on Ag<sub>2</sub>S quantum dots and graphitic carbon nitride nanosheets for the fluorescent detection of Cerium. *Talanta* **2019**, *200*, 249–255. [[CrossRef](#)]
43. Chen, T.H.; Tseng, W.L. Self-assembly of monodisperse carbon dots into high-brightness nanoaggregates for cellular uptake imaging and iron(III) sensing. *Anal. Chem.* **2017**, *89*, 11348–11356. [[CrossRef](#)]
44. Li, Z.; Guo, S.; Yuan, Z.; Lu, C. Carbon quantum dot-gold nanocluster nanosatellite for ratiometric fluorescence probe and imaging for hydrogen peroxide in living cells. *Sens. Actuators B Chem.* **2017**, *241*, 821–827. [[CrossRef](#)]
45. Yan, X.; Chen, Z.; Huang, Y.; Kang, C.; Yu, R. Generalized ratiometric fluorescence nanosensors based on carbon dots and an advanced chemometric model. *Talanta* **2019**, *192*, 233–240. [[CrossRef](#)] [[PubMed](#)]
46. Chen, Y.; Zhao, C.; Wang, Y.; Rao, H.; Lu, Z.; Lu, C.; Shan, Z.; Ren, B.; Wu, W.; Wang, X. Green and high-yield synthesis of carbon dots for ratiometric fluorescent determination of pH and enzyme reactions. *Mater. Sci. Eng. C* **2020**, *117*, 111264. [[CrossRef](#)] [[PubMed](#)]
47. He, Y.; Pan, C.; Cao, H.; Yue, M.; Wang, L.; Liang, G. Highly sensitive and selective dual-emission ratiometric fluorescence detection of dopamine based on carbon dots-gold nanoclusters hybrid. *Sens. Actuators B Chem.* **2018**, *265*, 371–377. [[CrossRef](#)]
48. Shangguan, J.; He, D.; He, X.; Wang, K.; Xu, F.; Liu, J.; Tang, J.; Yang, X.; Huang, J. Label-free carbon-dots-based ratiometric fluorescence pH nanoprobe for intracellular pH sensing. *Anal. Chem.* **2016**, *88*, 7837–7843. [[CrossRef](#)] [[PubMed](#)]
49. Wang, Y.; Lu, L.; Peng, H.; Xu, J.; Wang, F.; Qi, R.; Xu, Z.; Zhang, W. Multi-doped carbon dots with ratiometric pH sensing properties for monitoring enzyme catalytic reactions. *Chem. Commun.* **2016**, *52*, 9247–9250. [[CrossRef](#)] [[PubMed](#)]
50. Liu, L.; Chen, L.; Liang, J.; Liu, L.; Han, H. A novel ratiometric probe based on nitrogen-doped carbon dots and rhodamine B isothiocyanate for detection of Fe<sup>3+</sup> in aqueous solution. *J. Anal. Methods Chem.* **2016**, *2016*, 4939582. [[CrossRef](#)] [[PubMed](#)]
51. Liu, J.; Dong, Y.; Ma, Y.; Han, Y.; Ma, S.; Chen, H.; Chen, X. One-step synthesis of red/green dual-emissive carbon dots for ratiometric sensitive ONOO<sup>-</sup> probing and cell imaging. *Nanoscale* **2018**, *10*, 13589–13598. [[CrossRef](#)]
52. Liu, P.; Liu, J.; Xu, Y. Ratiometric fluorescence determination of hydrogen peroxide using carbon dot-embedded Ag@EuWO<sub>4</sub>(OH) nanocomposites. *Microchim. Acta* **2020**, *187*, 369. [[CrossRef](#)]
53. Molla, A.; Lee, H.; Ju, Y.; Choi, J.; Kim, J. Ratiometric fluorescence probe based on monochromatic dual-emission carbon nanodots with fluorescence spectral change. *Dye. Pigm.* **2022**, *197*, 109883. [[CrossRef](#)]
54. Wang, H.; Zhang, P.; Tian, Y.; Zhang, Y.; Yang, H.; Chen, S.; Zeng, R.; Long, Y.; Chen, J. Real-time monitoring of endogenous cysteine levels in living cells using a CD-based ratiometric fluorescent nanoprobe. *Anal. Bioanal. Chem.* **2018**, *410*, 4379–4386. [[CrossRef](#)] [[PubMed](#)]
55. Lei, X.; Fu, Y.; Wu, Y.; Chen, L.; Liang, J. A ratiometric fluorescent probe for pH detection based on Ag<sub>2</sub>S quantum dots-carbon dots nanohybrids. *R. Soc. Open Sci.* **2020**, *7*, 200482. [[CrossRef](#)] [[PubMed](#)]
56. Lu, H.; Xu, S. Visualizing BPA by molecularly imprinted ratiometric fluorescence sensor based on dual emission nanoparticles. *Biosens. Bioelectron.* **2017**, *92*, 147–153. [[CrossRef](#)]
57. Chen, B.; Liu, M.; Gao, Y.; Chang, S.; Qian, R.; Li, D. Design and applications of carbon dots-based ratiometric fluorescent probes: A review. *Nano Res.* **2023**, *16*, 1064–1083. [[CrossRef](#)]
58. Yang, X.; Li, C.; Li, P.; Fu, Q. Ratiometric optical probes for biosensing. *Theranostics* **2023**, *13*, 2632–2656. [[CrossRef](#)]
59. Xu, Y.; Wang, C.; Zhuo, H.; Zhou, D.; Song, Q. The function-oriented precursor selection for the preparation of carbon dots. *Nano Res.* **2023**, *16*, 11221–11249. [[CrossRef](#)]
60. Yan, F.; Bai, Z.; Liu, F.; Zu, F.; Zhang, R.; Xu, J.; Chen, L. Ratiometric fluorescence probes based on carbon dots. *Curr. Org. Chem.* **2018**, *22*, 57–66. [[CrossRef](#)]
61. Gui, R.; Jin, H.; Bu, X.; Fu, Y.; Wang, Z.; Liu, Q. Recent advances in dual-emission ratiometric fluorescence probes for chemo/biosensing and bioimaging of biomarkers. *Coord. Chem. Rev.* **2019**, *383*, 82–103. [[CrossRef](#)]



62. Han, Y.; Yang, W.; Luo, X.; He, X.; Zhao, H.; Tang, W.; Yue, T.; Li, Z. Carbon dots based ratiometric fluorescent sensing platform for food safety. *Crit. Rev. Food Sci. Nutr.* **2022**, *62*, 244–260. [[CrossRef](#)]
63. Zhang, J.; Chen, H.; Xu, K.; Deng, D.; Zhang, Q.; Luo, L. Current progress of ratiometric fluorescence sensors based on carbon dots in foodborne contaminant detection. *Biosensors* **2023**, *13*, 233. [[CrossRef](#)] [[PubMed](#)]
64. Chang, D.; Zhao, Z.; Shi, H.; Feng, J.; Yang, Y.; Shi, L. Ratiometric fluorescent carbon dots for enantioselective sensing of L-lysine and pH discrimination in vivo and in vitro. *Sens. Actuators B Chem.* **2022**, *362*, 131792. [[CrossRef](#)]
65. Shen, Z.; Zhang, C.; Yu, X.; Li, J.; Wang, Z.; Zhang, Z.; Liu, B. Microwave-assisted synthesis of cyclen functional carbon dots to construct a ratiometric fluorescent probe for tetracycline detection. *J. Mater. Chem. C* **2018**, *6*, 9636–9641. [[CrossRef](#)]
66. Yu, C.; Li, X.; Zeng, F.; Zheng, F.; Wu, S. Carbon-dot-based ratiometric fluorescent sensor for detecting hydrogen sulfide in aqueous media and inside live cells. *Chem. Commun.* **2013**, *49*, 403–405. [[CrossRef](#)] [[PubMed](#)]
67. Wang, L.; Cao, H.; He, Y.; Pan, C.; Sun, T.; Zhang, X.; Wang, C.; Liang, G. Facile preparation of amino-carbon dots/gold nanoclusters FRET ratiometric fluorescent probe for sensing of  $Pb^{2+}/Cu^{2+}$ . *Sens. Actuators B Chem.* **2019**, *282*, 78–84. [[CrossRef](#)]
68. Tao, H.; Zhang, Z.; Cao, Q.; Li, L.; Xu, S.; Jiang, C.; Li, Y.; Liu, Y. Ratiometric fluorescent sensors for nitrite detection in the environment based on carbon dot/Rhodamine B systems. *RSC Adv.* **2022**, *12*, 12655–12662. [[CrossRef](#)] [[PubMed](#)]
69. Yu, B.; Wang, Y.; Sun, M.; Luo, Y.; Yu, H.; Zhang, L. Preparation of carbon dots-doped terbium phosphonate coordination polymers as ratiometric fluorescent probe for citrate detection. *Spectrochim. Acta Part A* **2022**, *268*, 120656. [[CrossRef](#)] [[PubMed](#)]
70. Huang, J.; Li, F.; Guo, R.; Chen, Y.; Wang, Z.; Zhang, C.; Zheng, Y.; Weng, S.; Lin, X. A signal-on ratiometric fluorometric heparin assay based on the direct interaction between amino-modified carbon dots and DNA. *Microchim. Acta* **2018**, *185*, 260. [[CrossRef](#)]
71. Hao, T.; Wei, X.; Nie, Y.; Xu, Y.; Lu, K.; Yan, Y.; Zhou, Z. Surface modification and ratiometric fluorescence dual function enhancement for visual and fluorescent detection of glucose based on dual-emission quantum dots hybrid. *Sens. Actuators B Chem.* **2016**, *230*, 70–76. [[CrossRef](#)]
72. Gui, R.; Bu, X.; He, W.; Jin, H. Ratiometric fluorescence, solution-phase and filter-paper visualization detection of ciprofloxacin based on dual-emitting carbon dot/silicon dot hybrids. *New J. Chem.* **2018**, *42*, 16217–16225. [[CrossRef](#)]
73. Song, W.; Duan, W.; Liu, Y.; Ye, Z.; Chen, Y.; Chen, H.; Qi, S.; Wu, J.; Liu, D.; Xiao, L.; et al. Ratiometric detection of intracellular lysine and pH with one-pot synthesized dual emissive carbon dots. *Anal. Chem.* **2017**, *89*, 13626–13633. [[CrossRef](#)] [[PubMed](#)]
74. Xu, S.; He, X.; Huang, Y.; Liu, X.; Zhao, L.; Wang, X.; Sun, Y.; Ma, P.; Song, D. Lysosome-targeted ratiometric fluorescent sensor for monitoring pH in living cells based on one-pot-synthesized carbon dots. *Microchim. Acta* **2020**, *187*, 478. [[CrossRef](#)] [[PubMed](#)]
75. Wang, J.; Li, D.; Qiu, Y.; Liu, X.; Huang, L.; Wen, H.; Hu, J. An europium functionalized carbon dot-based fluorescence test paper for visual and quantitative point-of-care testing of anthrax biomarker. *Talanta* **2020**, *220*, 121377. [[CrossRef](#)]
76. Bu, X.; Fu, Y.; Jiang, X.; Jin, H.; Gui, R. Self-assembly of DNA-templated copper nanoclusters and carbon dots for ratiometric fluorometric and visual determination of arginine and acetaminophen with a logic-gate operation. *Microchim. Acta* **2020**, *187*, 154. [[CrossRef](#)]
77. Hu, S.R.; Yang, C.R.; Huang, Y.F.; Huang, C.C.; Chen, Y.L.; Chang, H.T. Ratiometric fluorescence probe of vesicle-like carbon dots and gold clusters for quantitation of cholesterol. *Chemosensors* **2022**, *10*, 160. [[CrossRef](#)]
78. An, J.; Chen, R.; Chen, M.; Hu, Y.; Lyu, Y.; Liu, Y. An ultrasensitive turn-on ratiometric fluorescent probes for detection of  $Ag^+$  based on carbon dots/ $SiO_2$  and gold nanoclusters. *Sens. Actuators B Chem.* **2021**, *329*, 129097. [[CrossRef](#)]
79. Zhou, W.; Hu, Z.; Wei, J.; Lu, H.; Dai, H.; Zhao, J.; Zhang, W.; Guo, R. A ratiometric fluorescent probe based on PCN-224 for rapid and ultrasensitive detection of copper ions. *Compos. Commun.* **2022**, *33*, 101221. [[CrossRef](#)]
80. Gong, W.; Nan, H.; Peng, H.; Wang, Y.; Dong, Z.; Zhang, Z.; Cao, X.; Liu, Y. A ratiometric fluorescent sensor for  $UO_2^{2+}$  detection based on  $Ag^+$ -modified gold nanoclusters hybrid via photoinduced electron transfer (PET) mechanism. *Microchem. J.* **2023**, *190*, 108725. [[CrossRef](#)]
81. Chen, X.; Luan, Y.; Wang, N.; Zhou, Z.; Ni, X.; Cao, Y.; Zhang, G.; Lai, Y.; Yang, W. Ratiometric fluorescence nanosensors based on core-shell structured carbon/CdTe quantum dots and surface molecularly imprinted polymers for the detection of sulfadiazine. *J. Sep. Sci.* **2018**, *41*, 4394–4401. [[CrossRef](#)]
82. Heng, H.; Ma, D.; Gu, Q.; Li, J.; Jin, H.; Shen, P.; Wei, J.; Wang, Z. A core-shell structure ratiometric fluorescent probe based on carbon dots and  $Tb^{3+}$  for the detection of anthrax biomarker. *Spectrochim. Acta Part A* **2023**, *299*, 122793. [[CrossRef](#)] [[PubMed](#)]
83. Ran, H.; Lin, Z.; Hong, C.; Zeng, J.; Yao, Q.; Huang, Z. Self-assembly PS@dual-emission ratiometric fluorescence probe coupled with core-shell structured MIP for the detection of malachite green in fish. *J. Photochem. Photobiol. A* **2019**, *372*, 260–269. [[CrossRef](#)]
84. Liu, M.; Gao, Z.; Yu, Y.; Su, R.; Huang, R.; Qi, W.; He, Z. Molecularly imprinted core-shell  $CdSe@SiO_2/CDs$  as a ratiometric fluorescent probe for 4-nitrophenol sensing. *Nanoscale Res. Lett.* **2018**, *13*, 27. [[CrossRef](#)]
85. Lu, H.; Yu, C.; Zhang, Y.; Xu, S. Efficient core shell structured dual response ratiometric fluorescence probe for determination of  $H_2O_2$  and glucose via etching of silver nanoprisms. *Anal. Chim. Acta* **2019**, *1048*, 178–185. [[CrossRef](#)]
86. Ghasemi, F.; Hormozi-Nezhad, M.R.; Mahmoudi, M. A new strategy to design colorful ratiometric probes and its application to fluorescent detection of  $Hg(II)$ . *Sens. Actuators B Chem.* **2018**, *259*, 894–899. [[CrossRef](#)]
87. Zhang, Z.; Tao, H.; Cao, Q.; Li, L.; Xu, S.; Li, Y.; Liu, Y. Ratiometric fluorescence sensor for sensitive detection of inorganic phosphate in environmental samples. *Anal. Bioanal. Chem.* **2022**, *414*, 3507–3515. [[CrossRef](#)] [[PubMed](#)]
88. Qin, L.; Guo, Y.; Li, L.; Lin, D.; Li, Y.; Xu, S.; Jiang, C. Ratiometric fluorescent sensor based on hydrogen-bond triggering the internal filter effect for enzyme-free and visual monitoring pesticide residues. *ACS Sustain. Chem. Eng.* **2023**, *11*, 11032–11040. [[CrossRef](#)]

89. Chen, P.; Xu, X.; Ji, J.; Wu, J.; Lu, T.; Xia, Y.; Wang, L.; Fan, J.; Jin, Y.; Zhang, L.; et al. Specific and visual assay of iodide ion in human urine via redox pretreatment using ratiometric fluorescent test paper printed with dimer DNA silver nanoclusters and carbon dots. *Anal. Chim. Acta* **2020**, *1138*, 99–107. [[CrossRef](#)]
90. Qu, Z.; Yu, T.; Bi, L. A dual-channel ratiometric fluorescent probe for determination of the activity of tyrosinase using nitrogen-doped graphene quantum dots and dopamine-modified CdTe quantum dots. *Microchim. Acta* **2019**, *186*, 635. [[CrossRef](#)]
91. Ma, Y.; Wang, Y.; Liu, Y.; Shi, L.; Yang, D. Multi-carbon dots and aptamer based signal amplification ratiometric fluorescence probe for protein tyrosine kinase 7 detection. *J. Nanobiotechnol.* **2021**, *19*, 47. [[CrossRef](#)]
92. Liu, C.; Ning, D.; Zhang, C.; Liu, Z.; Zhang, R.; Zhao, J.; Zhao, T.; Liu, B.; Zhang, Z. Dual-colored carbon dot ratiometric fluorescent test paper based on a specific spectral energy transfer for semiquantitative assay of copper ions. *ACS Appl. Mater. Interfaces* **2017**, *9*, 18897–18903. [[CrossRef](#)] [[PubMed](#)]
93. He, Y.; Yu, Z.; He, J.; Zhang, H.; Liu, Y.; Lei, B. Ratiometric and selective fluorescent sensor for Fe(III) and bovine serum albumin based on energy transfer. *Sens. Actuators B Chem.* **2018**, *262*, 228–235. [[CrossRef](#)]
94. Sun, X.; Cai, L.; He, W.; Cao, X.; Liu, B.; Wang, H. A novel ratiometric fluorescent probe for water content in ethanol and temperature sensing. *Spectrochim. Acta Part A* **2022**, *264*, 120266. [[CrossRef](#)] [[PubMed](#)]
95. Xu, Y.; Wei, X.; Li, H.; Zheng, X.; Lu, K.; Liu, X.; Wang, K.; Yan, Y. Boric acid functionalized ratiometric fluorescence probe for sensitive and on-site naked eye determination of dopamine based on two different kinds of quantum dots. *RSC Adv.* **2016**, *6*, 72715–72721. [[CrossRef](#)]
96. Xiao, W.; Liu, F.; Yan, G.; Shi, W.; Peng, K.; Yang, X.; Li, X.; Yu, H.; Shi, Z.; Zeng, H. Yttrium vanadates based ratiometric fluorescence probe for alkaline phosphatase activity sensing. *Colloids Surf. B* **2020**, *185*, 110618. [[CrossRef](#)]
97. Yang, S.; Guo, W.; Sun, X. Electrostatic association complex of a polymer capped CdTe(S) quantum dot and a small molecule dye as a robust ratiometric fluorescence probe of copper ions. *Dye. Pigm.* **2018**, *158*, 114–120. [[CrossRef](#)]
98. Paydar, S.; Feizi, F.; Shamsipur, M.; Barati, A.; Chehri, N.; Taherpour, A.; Jamshidi, M. An ideal ratiometric fluorescent probe provided by the surface modification of carbon dots for the determination of Pb<sup>2+</sup>. *Sens. Actuators B Chem.* **2022**, *369*, 132243. [[CrossRef](#)]
99. Chen, S.; Li, S.; Liu, X.; Shi, B.; Huang, Y.; Zhao, S. Nitrogen and sulfur co-doped carbon dot-based ratiometric fluorescent probe for Zn<sup>2+</sup> sensing and imaging in living cells. *Microchim. Acta* **2022**, *189*, 107. [[CrossRef](#)]
100. Chen, Z.; Xu, X.; Meng, D.; Jiang, H.; Zhou, Y.; Feng, S.; Mu, Z.; Yang, Y. Dual-emitting N/S-doped carbon dots-based ratiometric fluorescent and light scattering sensor for high precision detection of Fe(III) ions. *J. Fluoresc.* **2020**, *30*, 1007–1013. [[CrossRef](#)]
101. Zheng, Y.; Wan, Y.; Wei, Y.; Yu, Y. One-pot synthesis of dual-emissive carbon dots for ratiometric fluorescent determination of Hg<sup>2+</sup>. *J. Fluoresc.* **2023**, *33*, 1941–1948. [[CrossRef](#)]
102. Lu, W.; Liu, Y.; Zhang, Z.; Xiao, J.; Liu, C. Dual emissive amphiphilic carbon dots as ratiometric fluorescent probes for the determination of critical micelle concentration of surfactants. *Anal. Methods* **2022**, *14*, 672–677. [[CrossRef](#)]
103. Zheng, Y.; Li, C.; Li, Q.; Zhang, T.; Chen, J.; Ji, W.; Wei, Y. A ratiometric probe based on carbon dots and calcein & Eu<sup>3+</sup> for the fluorescent detection of sodium tripolyphosphate. *J. Fluoresc.* **2023**, *33*, 965–972. [[PubMed](#)]
104. Pang, S.; Liu, S. Dual-emission carbon dots for ratiometric detection of Fe<sup>3+</sup> ions and acid phosphatase. *Anal. Chim. Acta* **2020**, *1105*, 155–161. [[CrossRef](#)] [[PubMed](#)]
105. Liu, L.; Chen, M.; Yuan, L.; Mi, Z.; Li, C.; Liu, Z.; Chen, Z.; Wang, L.; Feng, F.; Wu, L. A novel ratiometric fluorescent probe based on dual-emission carbon dots for highly sensitive detection of salicylic acid. *Spectrochim. Acta Part A* **2023**, *303*, 123232. [[CrossRef](#)] [[PubMed](#)]
106. Gao, Y.; Jiao, Y.; Zhang, H.; Lu, W.; Liu, Y.; Han, H.; Gong, X.; Li, L.; Shuang, S.; Dong, C. One-step synthesis of a dual-emitting carbon dot-based ratiometric fluorescent probe for the visual assay of Pb<sup>2+</sup> and PPI and development of a paper sensor. *J. Mater. Chem. B* **2019**, *7*, 5502–5509. [[CrossRef](#)] [[PubMed](#)]
107. Behzadifar, S.; Bagheri Pebdeni, A.; Hosseini, M.; Mohammadnejad, J. A new ratiometric fluorescent detection of Glucose-6-phosphate dehydrogenase enzyme based on dually emitting carbon dots and silver nanoparticles. *Microchem. J.* **2022**, *182*, 107947. [[CrossRef](#)]
108. Guo, L.; Song, Y.; Cai, K.; Wang, L. “On-off” ratiometric fluorescent detection of Hg<sup>2+</sup> based on N-doped carbon dots-rhodamine B@TAPT-DHTA-COF. *Spectrochim. Acta Part A* **2020**, *227*, 117703. [[CrossRef](#)] [[PubMed](#)]
109. Babae, E.; Barati, A.; Gholivand, M.B.; Taherpour, A.; Zolfaghar, N.; Shamsipur, M. Determination of Hg<sup>2+</sup> and Cu<sup>2+</sup> ions by dual-emissive Ag/Au nanocluster/carbon dots nanohybrids: Switching the selectivity by pH adjustment. *J. Hazard. Mater.* **2019**, *367*, 437–446. [[CrossRef](#)] [[PubMed](#)]
110. Guo, X.; Liu, C.; Li, N.; Zhang, S.; Wang, Z. Ratiometric fluorescent test paper based on silicon nanocrystals and carbon dots for sensitive determination of mercuric ions. *R. Soc. Open Sci.* **2018**, *5*, 171922. [[CrossRef](#)]
111. Liu, P.; Hao, R.; Sun, W.; Lin, Z.; Jing, T.; Yang, H. A “bottle-around-ship” method to encapsulated carbon nitride and CdTe quantum dots in ZIF-8 as the dual emission fluorescent probe for detection of mercury (II) ion. *Anal. Sci.* **2022**, *38*, 1305–1312. [[CrossRef](#)] [[PubMed](#)]
112. Cao, B.; Yuan, C.; Liu, B.; Jiang, C.; Guan, G.; Han, M. Ratiometric fluorescence detection of mercuric ion based on the nanohybrid of fluorescence carbon dots and quantum dots. *Anal. Chim. Acta* **2013**, *786*, 146–152. [[CrossRef](#)] [[PubMed](#)]

113. Huang, S.; Yao, J.; Ning, G.; Li, B.; Mu, P.; Xiao, Q. Ultrasensitive ratiometric fluorescent probes for Hg(II) and trypsin activity based on carbon dots and metalloporphyrin via a target recycling amplification strategy. *Analyst* **2022**, *147*, 1457–1466. [[CrossRef](#)] [[PubMed](#)]
114. Yan, Y.; Yu, H.; Zhang, K.; Sun, M.; Zhang, Y.; Wang, X.; Wang, S. Dual-emissive nanohybrid of carbon dots and gold nanoclusters for sensitive determination of mercuric ions. *Nano Res.* **2016**, *9*, 2088–2096. [[CrossRef](#)]
115. Jia, K.; Yi, K.; Zhang, W.; Yan, P.; Zhang, S.; Liu, X. Carbon nanodots calibrated fluorescent probe of QD@amphiphilic polyurethane for ratiometric detection of Hg (II). *Sens. Actuators B Chem.* **2022**, *370*, 132443. [[CrossRef](#)]
116. Li, W.; Hu, X.; Li, Q.; Shi, Y.; Zhai, X.; Xu, Y.; Li, Z.; Huang, X.; Wang, X.; Shi, J.; et al. Copper nanoclusters @ nitrogen-doped carbon quantum dots-based ratiometric fluorescence probe for lead (II) ions detection in porphyra. *Food Chem.* **2020**, *320*, 126623. [[CrossRef](#)]
117. Lu, H.; Yu, C.; Xu, S. A dual reference ion-imprinted ratiometric fluorescence probe for simultaneous detection of silver (I) and lead (II). *Sens. Actuators B Chem.* **2019**, *288*, 691–698. [[CrossRef](#)]
118. Yi, K.; Zhang, L. Embedding dual fluoroprobe in metal-organic frameworks for continuous visual recognition of Pb<sup>2+</sup> and PO<sub>4</sub><sup>3-</sup> via fluorescence ‘turn-off-on’ response: Agar test paper and fingerprint. *J. Hazard. Mater.* **2020**, *389*, 122141. [[CrossRef](#)] [[PubMed](#)]
119. Yao, C.; Dong, L.; Yang, L.; Wang, J.; Li, S.; Lv, H.; Ji, X.; Liu, J.; Wang, S. Integration of metal-organic frameworks with Bi-nanoprobes as dual-emissive ratiometric sensors for fast and highly sensitive determination of food hazards. *Molecules* **2022**, *27*, 2356. [[CrossRef](#)]
120. Ma, Y.; Chen, Y.; Liu, J.; Han, Y.; Ma, S.; Chen, X. Ratiometric fluorescent detection of chromium(VI) in real samples based on dual emissive carbon dots. *Talanta* **2018**, *185*, 249–257. [[CrossRef](#)]
121. Zhang, S.; Jin, L.; Liu, J.; Wang, Q.; Jiao, L. A label-free yellow-emissive carbon dot-based nanosensor for sensitive and selective ratiometric detection of chromium (VI) in environmental water samples. *Mater. Chem. Phys.* **2020**, *248*, 122912. [[CrossRef](#)]
122. Bogireddy, N.K.R.; Sotelo Rios, S.E.; Agarwal, V. Simple one step synthesis of dual-emissive heteroatom doped carbon dots for acetone sensing in commercial products and Cr (VI) reduction. *Chem. Eng. J.* **2021**, *414*, 128830. [[CrossRef](#)]
123. Mei, X.; Wang, D.; Wang, S.; Li, J.; Dong, C. Synthesis of intrinsic dual-emission type N,S-doped carbon dots for ratiometric fluorescence detection of Cr (VI) and application in cellular imaging. *Anal. Bioanal. Chem.* **2022**, *414*, 7253–7263. [[CrossRef](#)] [[PubMed](#)]
124. Yan, L.; Li, J.; Cai, H.; Shao, Y.; Zhang, G.; Chen, L.; Wang, Y.; Zong, H.; Yin, Y. Carbon dots/Ag nanoclusters-based fluorescent probe for ratiometric and visual detection of Cu<sup>2+</sup>. *J. Alloys Compd.* **2023**, *945*, 169227. [[CrossRef](#)]
125. Wang, Y.; Zhang, C.; Chen, X.; Yang, B.; Yang, L.; Jiang, C.; Zhang, Z. Ratiometric fluorescent paper sensor utilizing hybrid carbon dots–quantum dots for the visual determination of copper ions. *Nanoscale* **2016**, *8*, 5977–5984. [[CrossRef](#)] [[PubMed](#)]
126. Guo, J.; Liu, A.; Zeng, Y.; Cai, H.; Ye, S.; Li, H.; Yan, W.; Zhou, F.; Song, J.; Qu, J. Novel dual-emission fluorescence carbon dots as a ratiometric probe for Cu<sup>2+</sup> and ClO<sup>-</sup> detection. *Nanomaterials* **2021**, *11*, 1232. [[CrossRef](#)]
127. Luo, F.; Zhu, M.; Liu, Y.; Sun, J.; Gao, F. Ratiometric and visual determination of copper ions with fluorescent nanohybrids of semiconducting polymer nanoparticles and carbon dots. *Spectrochim. Acta Part A* **2023**, *295*, 122574. [[CrossRef](#)] [[PubMed](#)]
128. Zhang, H.; Li, Y.; Lu, H.; Gan, F. A ratiometric fluorescence and colorimetric dual-mode sensing platform based on sulfur quantum dots and carbon quantum dots for selective detection of Cu<sup>2+</sup>. *Anal. Bioanal. Chem.* **2022**, *414*, 2471–2480. [[CrossRef](#)] [[PubMed](#)]
129. Wang, S.; Guo, L.; Chen, L.; Wang, L.; Song, Y. Self-exfoliating double-emission N-doped carbon dots in covalent organic frameworks for ratiometric fluorescence “off-on” Cu<sup>2+</sup> detection. *ACS Appl. Nano Mater* **2022**, *5*, 1339–1347. [[CrossRef](#)]
130. Weerasinghe, J.; Scott, J.; Deshan, A.D.K.; Chen, D.; Singh, A.; Sen, S.; Sonar, P.; Vasilev, K.; Li, Q.; Ostrikov, K. Monochromatic blue and switchable blue-green carbon quantum dots by room-temperature air plasma processing. *Adv. Mater. Technol.* **2022**, *7*, 2100586. [[CrossRef](#)]
131. Wu, H.; Tong, C. Ratiometric fluorometric determination of silver(I) by using blue-emitting silicon- and nitrogen-doped carbon quantum dots and red-emitting N-acetyl-L-cysteine-capped CdTe quantum dots. *Microchim. Acta* **2019**, *186*, 723. [[CrossRef](#)] [[PubMed](#)]
132. Chang, J.; Mao, J.; Lu, Y.; Liu, Y.; Wang, S. Construction of ratiometric fluorescent nanosensors based on carbon dots dual emission strategy for high-sensitivity visual detection of Ag<sup>+</sup>. *Int. J. Environ. Anal. Chem.* **2023**, 1–15. [[CrossRef](#)]
133. You, J.; Ji, J.; Wu, J.; Wang, S.; Chen, P.; Mao, R.; Jin, Y.; Zhang, L.; Du, S. Ratiometric fluorescent test pen filled with a mixing ink of carbon dots and CdTe quantum dots for portable assay of silver ion on paper. *Microchim. Acta* **2020**, *187*, 391. [[CrossRef](#)] [[PubMed](#)]
134. Shokri, R.; Amjadi, M. A ratiometric fluorescence sensor for triticonazole based on the encapsulated boron-doped and phosphorous-doped carbon dots in the metal organic framework. *Spectrochim. Acta Part A* **2021**, *246*, 118951. [[CrossRef](#)]
135. Ma, Z.; Zhang, Y.; Ren, X.; He, X.; Li, W.; Zhang, Y. Dual-reverse-signal ratiometric fluorescence method for malachite green detection based on multi-mechanism synergistic effect. *Spectrochim. Acta Part A* **2022**, *276*, 121196. [[CrossRef](#)]
136. Mei, H.; Zhu, X.; Li, Z.; Jiang, J.; Wang, H.; Wang, X.; Zhou, P. Manganese dioxide nanosheet-modulated ratiometric fluoroprobe based on carbon quantum dots from okra for selective and sensitive dichlorvos detection in foods. *Food Chem.* **2024**, *434*, 137507. [[CrossRef](#)] [[PubMed](#)]

137. Wu, H.; Xu, M.; Chen, Y.; Zhang, H.; Shen, Y.; Tang, Y. A highly sensitive and selective nano-fluorescent probe for ratiometric and visual detection of oxytetracycline benefiting from dual roles of nitrogen-doped carbon dots. *Nanomaterials* **2022**, *12*, 4306. [[CrossRef](#)] [[PubMed](#)]
138. Guo, H.; Wang, X.; Wu, N.; Xu, M.; Wang, M.; Zhang, L.; Yang, W. In-situ synthesis of carbon dots-embedded europium metal-organic frameworks for ratiometric fluorescence detection of Hg<sup>2+</sup> in aqueous environment. *Anal. Chim. Acta* **2021**, *1141*, 13–20. [[CrossRef](#)]
139. Hu, F.; Fu, Q.; Li, Y.; Yan, C.; Xiao, D.; Ju, P.; Hu, Z.; Li, H.; Ai, S. Zinc-doped carbon quantum dots-based ratiometric fluorescence probe for rapid, specific, and visual determination of tetracycline hydrochloride. *Food Chem.* **2024**, *431*, 137097. [[CrossRef](#)]
140. Liu, Y.; Cao, Y.; Bu, T.; Sun, X.; Zhe, T.; Huang, C.; Yao, S.; Wang, L. Silicon-doped carbon quantum dots with blue and green emission are a viable ratiometric fluorescent probe for hydroquinone. *Microchim. Acta* **2019**, *186*, 399. [[CrossRef](#)]
141. Jalili, R.; Khataee, A. Application of molecularly imprinted polymers and dual-emission carbon dots hybrid for ratiometric determination of chloramphenicol in milk. *Food Chem. Toxicol.* **2020**, *146*, 111806. [[CrossRef](#)]
142. Lu, C.; Liu, G.; Yang, Z.; Wang, Y.; Rao, H.; Zhang, W.; Jing, B.; Wang, X. A ratiometric fluorometric ciprofloxacin assay based on the use of riboflavin and carbon dots. *Microchim. Acta* **2019**, *187*, 37. [[CrossRef](#)] [[PubMed](#)]
143. Fan, Y.; Shen, L.; Liu, Y.; Hu, Y.; Long, W.; Fu, H.; She, Y. A sensitized ratiometric fluorescence probe based on N/S doped carbon dots and mercaptoacetic acid capped CdTe quantum dots for the highly selective detection of multiple tetracycline antibiotics in food. *Food Chem.* **2023**, *421*, 136105. [[CrossRef](#)]
144. Rao, H.; Dai, Y.; Ge, H.; Liu, X.; Chen, B.; Zou, P.; Wang, X.; Wang, Y. Visual and fluorescence detection of pyrogallol based on a ratiometric fluorescence-enzyme system. *New J. Chem.* **2017**, *41*, 6630–6637. [[CrossRef](#)]
145. Fan, Y.J.; Su, M.; Shi, Y.E.; Liu, X.T.; Shen, S.G.; Dong, J.X. A ratiometric fluorescent sensor for tetracyclines detection in meat based on pH-dependence of targets with lanthanum-doped carbon dots as probes. *Anal. Bioanal. Chem.* **2022**, *414*, 2597–2606. [[CrossRef](#)]
146. Yang, G.; Zhang, J.; Gu, L.; Tang, Y.; Zhang, X.; Huang, X.; Shen, X.; Zhai, W.; Fodjo, E.K.; Kong, C. Ratiometric fluorescence immunoassay based on carbon quantum dots for sensitive detection of malachite green in fish. *Biosensors* **2023**, *13*, 38. [[CrossRef](#)]
147. Sun, X.; Jiang, M.; Chen, L.; Niu, N. Construction of ratiometric fluorescence MIPs probe for selective detection of tetracycline based on passion fruit peel carbon dots and europium. *Microchim. Acta* **2021**, *188*, 297. [[CrossRef](#)] [[PubMed](#)]
148. Zhang, L.; Xing, H.; Liu, W.; Wang, Z.; Hao, Y.; Wang, H.; Dong, W.; Liu, Y.; Shuang, S.; Dong, C.; et al. 11-Mercaptoundecanoic acid-functionalized carbon dots as a ratiometric optical probe for doxorubicin detection. *ACS Appl. Nano Mater* **2021**, *4*, 13734–13746. [[CrossRef](#)]
149. Chen, A.; Li, R.; Zhong, Y.; Deng, Q.; Yin, X.; Li, H.; Kong, L.; Yang, R. A novel chiral fluorescence probe based on carbon dots-copper(II) system for ratio fluorescence detection of gatifloxacin. *Sens. Actuators B Chem.* **2022**, *359*, 131602. [[CrossRef](#)]
150. Xiang, G.; Ren, Y.; Xia, Y.; Mao, W.; Fan, C.; Guo, S.; Wang, P.; Yang, D.; He, L.; Jiang, X. Carbon-dot-based dual-emission silica nanoparticles as a ratiometric fluorescent probe for bisphenol A. *Spectrochim. Acta Part A* **2017**, *177*, 153–157. [[CrossRef](#)]
151. Shen, J.; Fan, Z. Construction of nanohybrid Tb@CDs/GSH-CuNCs as a ratiometric probe to detect phosphate anion based on aggregation-induced emission and FRET mechanism. *Microchim. Acta* **2023**, *190*, 427. [[CrossRef](#)] [[PubMed](#)]
152. Zhan, Y.; Zeng, Y.; Li, L.; Luo, F.; Qiu, B.; Lin, Z.; Guo, L. Ratiometric fluorescent hydrogel test kit for on-spot visual detection of nitrite. *ACS Sens.* **2019**, *4*, 1252–1260. [[CrossRef](#)] [[PubMed](#)]
153. Qi, W.; Chen, L.; Du, C.; Wang, Y. A ratiometric fluorescence probe of dopamine-functionalized carbon nanodots for hypochlorite detection. *Chemosensors* **2022**, *10*, 383. [[CrossRef](#)]
154. Zhang, H.; Gao, Y.; Jiao, Y.; Lu, W.; Shuang, S.; Dong, C. Highly sensitive fluorescent carbon dots probe with ratiometric emission for the determination of ClO<sup>-</sup>. *Analyst* **2020**, *145*, 2212–2218. [[CrossRef](#)] [[PubMed](#)]
155. Peng, L.; Yang, M.; Zhang, M.; Jia, M. A ratiometric fluorescent sensor based on carbon dots for rapid determination of bisulfite in sugar. *Food Chem.* **2022**, *392*, 133265. [[CrossRef](#)] [[PubMed](#)]
156. Liang, M.; Chen, Y.; Zhang, H.; Niu, X.; Xu, L.; Ren, C.; Chen, X. Fluorescence resonance energy transfer-based ratiometric fluorescent assay for highly sensitive and selective determination of sulfide anions. *Analyst* **2015**, *140*, 6711–6719. [[CrossRef](#)] [[PubMed](#)]
157. He, Y.; He, J.; Wang, L.; Yu, Z.; Zhang, H.; Liu, Y.; Lei, B. Synthesis of double carbon dots co-doped mesoporous Al<sub>2</sub>O<sub>3</sub> for ratiometric fluorescent determination of oxygen. *Sens. Actuators B Chem.* **2017**, *251*, 918–926. [[CrossRef](#)]
158. Gao, J.; Li, Q.; Wang, C.; Tan, H. Copper (II)-mediated fluorescence of lanthanide coordination polymers doped with carbon dots for ratiometric detection of hydrogen sulfide. *Sens. Actuators B Chem.* **2017**, *253*, 27–33. [[CrossRef](#)]
159. Zou, G.Y.; Guo, L.; Chen, S.; Liu, N.Z.; Yu, Y.L. Multifunctional ratiometric fluorescent sensing platform constructed by grafting various response groups on carbon dots with bromine active site for biosensing and bioimaging. *Sens. Actuators B Chem.* **2022**, *357*, 131376. [[CrossRef](#)]
160. He, Q.; Zhuang, S.; Yu, Y.; Li, H.; Liu, Y. Ratiometric dual-emission of Rhodamine-B grafted carbon dots for full-range solvent components detection. *Anal. Chim. Acta* **2021**, *1174*, 338743. [[CrossRef](#)]
161. Yang, F.; Lin, D.; Pan, L.; Zhu, J.; Shen, J.; Yang, L.; Jiang, C. Portable smartphone platform based on a single dual-emissive ratiometric fluorescent probe for visual detection of isopropanol in exhaled breath. *Anal. Chem.* **2021**, *93*, 14506–14513. [[CrossRef](#)]
162. Yan, Y.; Sun, J.; Zhang, K.; Zhu, H.; Yu, H.; Sun, M.; Huang, D.; Wang, S. Visualizing gaseous nitrogen dioxide by ratiometric fluorescence of carbon nanodots-quantum dots hybrid. *Anal. Chem.* **2015**, *87*, 2087–2093. [[CrossRef](#)]

163. Shen, Y.; Wu, T.; Zhang, Y.; Ling, N.; Zheng, L.; Zhang, S.; Sun, Y.; Wang, X.; Ye, Y. Engineering of a dual-recognition ratiometric fluorescent nanosensor with a remarkably large Stokes shift for accurate tracking of pathogenic bacteria at the single-cell level. *Anal. Chem.* **2020**, *92*, 13396–13404. [[CrossRef](#)]
164. Li, X.; Wu, J.; Hu, H.; Liu, F.; Wang, J. A smartphone integrated platform for ratiometric fluorescent sensitive and selective determination of dipicolinic acid. *Biosensors* **2022**, *12*, 668. [[CrossRef](#)]
165. Qin, S.; Yan, B. Dual-emissive ratiometric fluorescent probe based on  $\text{Eu}^{3+}$ /C-dots@MOF hybrids for the biomarker diamino-toluene sensing. *Sens. Actuators B Chem.* **2018**, *272*, 510–517. [[CrossRef](#)]
166. Xu, X.; He, L.; Long, Y.; Pan, S.; Liu, H.; Yang, J.; Hu, X. S-doped carbon dots capped ZnCdTe quantum dots for ratiometric fluorescence sensing of guanine. *Sens. Actuators B Chem.* **2019**, *279*, 44–52. [[CrossRef](#)]
167. Zhang, T.; Gan, Z.; Zhen, S.; Hu, Y.; Hu, X. Ratiometric fluorescent probe based on carbon dots and Zn-doped CdTe QDs for detection of 6-Mercaptopurine. *Opt. Mater.* **2022**, *134*, 113196. [[CrossRef](#)]
168. Guo, R.; Chen, B.; Li, F.; Weng, S.; Zheng, Z.; Chen, M.; Wu, W.; Lin, X.; Yang, C. Positive carbon dots with dual roles of nanoquencher and reference signal for the ratiometric fluorescence sensing of DNA. *Sens. Actuators B Chem.* **2018**, *264*, 193–201. [[CrossRef](#)]
169. Miao, L.; Jiao, L.; Tang, Q.; Li, H.; Zhang, L.; Wei, Q. A nanozyme-linked immunosorbent assay for dual-modal colorimetric and ratiometric fluorescent detection of cardiac troponin I. *Sens. Actuators B Chem.* **2019**, *288*, 60–64. [[CrossRef](#)]
170. Zhan, Z.; Mao, H.; Xue, M.; Han, G.; Zhou, G.; Zhang, Y. Ratiometric fluorescence detection of the angiotensin-converting enzyme via single-excitation and double-emission biomass-derived carbon quantum dots. *Methods Appl. Fluoresc.* **2024**, *12*, 015004. [[CrossRef](#)] [[PubMed](#)]

**Disclaimer/Publisher's Note:** The statements, opinions and data contained in all publications are solely those of the individual author(s) and contributor(s) and not of MDPI and/or the editor(s). MDPI and/or the editor(s) disclaim responsibility for any injury to people or property resulting from any ideas, methods, instructions or products referred to in the content.